AEROSPACE INFORMATION REPORT

AIR5866™	REV. A
Issued 2008-02 Stabilized 2021-02 Superseding AIR5866	

An Assessment of Planar Waves

RATIONALE

This document contains information that is fundamental to the discipline of inlet-engine compatibility and is expected to remain stable for the foreseeable future.

STABILIZED NOTICE

This document has been declared "Stabilized" by the SAE S-16 Turbine Engine Inlet Flow Distortion Committee and will no longer be subjected to periodic reviews for currency. Users are responsible for verifying references and continued suitability of technical requirements. Newer technology may exist.

TO PLACE A DOCUMENT ORDER: **Tel: 877-606-7323 (inside USA and Canada)**
Tel: +1 724-776-4970 (outside USA)
Fax: 724-776-0790
Email: CustomerService@sae.org
SAE WEB ADDRESS: **http://www.sae.org**

For more information on this standard, visit
https://www.sae.org/standards/content/AIR5866A/

FOREWORD

As applications for turbine engines have become more sophisticated and the operating conditions more severe, inlet planar time-variant full-face total-pressure variations, usually accompanied by spatial total pressure distortion, can become a significant destabilizing factor. The SAE S-16 Turbine Engine Inlet Flow Distortion Committee has recognized the need for guidelines and procedures that would address inlet planar waves and the desirability of documentation similar to SAE documents ARP1420 and AIR1419 that were written for inlet spatial total-pressure distortion.

This Aerospace Information Report (AIR) brings together information and ideas that are required to address the planar wave problem. A common industry practice has yet to be established.

TABLE OF CONTENTS

1. SCOPE

“An Assessment of Planar Waves” provides background on some of the history of planar waves, which are time-dependent variations of inlet recovery, as well as establishing a hierarchy for categorizing various types of planar waves. It further identifies approaches for establishing compression-component and engine sensitivities to planar waves, and methods for accounting for the destabilizing effects of planar waves. This document contains an extensive list and categorization (see Appendix A) of references to aid both the newcomer and the practitioner on this subject.

The committee acknowledges that this document addresses only the impact of planar waves on compression-component stability and does not address the impact of planar waves on augmenter rumble, engine structural issues, and/or pilot discomfort.

2. REFERENCES

The references for this document encompass SAE publications, papers and reports to support the material in the body of the report, and papers and reports that were reviewed and may be sources for added insight for the interested reader.

2.1 Applicable Documents

The following publications form a part of this document to the extent specified herein. The latest issue of SAE publications shall apply. In the event of conflict between the text of this document and references cited herein, the text of this document takes precedence. Nothing in this document, however, supersedes applicable laws and regulations unless a specific exemption has been obtained.

2.1.1 SAE Publications

Available from SAE International, 400 Commonwealth Drive, Warrendale, PA 15096-0001, Tel: 877-606-7323 (inside USA and Canada) or 724-776-4970 (outside USA), www.sae.org.

2.1.1.1 ARP1420, “Gas Turbine Engine Inlet Flow Distortion Guidelines.”

2.1.1.2 AIR1419, “Inlet Total-Pressure Distortion Considerations for Gas-Turbine Engines.”

2.1.1.3 ARD500015, "A Current Assessment of the Inlet/Engine Temperature Distortion Problem" and to be republished as AIR5867, “An Assessment of the Inlet/Engine Temperature Distortion Problem.”

2.2 Other Applicable References

2.2.1 MacMiller, C. J. and Haagenson, W. R., “Unsteady Inlet Distortion Characteristics with the B-1B,” NA-86-1490A, presented at the 68th(A) Specialists Meeting of the AGARD Propulsion and Energetics Panel on Engine Response to Distorted Inflow Conditions, Munich, Germany, September 8-9, 1986.

2.2.2 Burstadt, P. L. and L. M. Wenzel, AIAA 76-703, “A Method to Account for Variations of Average Compressor Inlet Pressure During Instantaneous Distortion Analysis,” July 1976.

2.2.3 Willoh, R. H. and Seldner, K., NASA TM X-1880, “Multistage Compressor Simulation Applied to the Prediction of Axial Flow Instabilities,” NASA, September 1969.

2.2.4 Davis, M. W., ASME 82-GT-189, “A Stage-by-Stage Dual Spool Compression System Modeling Technique.”

2.2.5 Reynolds, G. G. and W. G. Steenken, AFAPL-TR-76-76, “Dynamic Digital Blade Row Compression Component Stability Model - Model Validation and Analysis of Planar Pulse Generator and Two-Stage Fan Test Data,” AFAPL, August 1976.

2.2.6 Tesch, W. A., R. E. Moszee and W. G. Steenken, NASA CR-135162, “Linearized Blade Row Compression Component Model - Stability and Frequency Response Analysis of a J85-13 Compressor”, NASA, September 1976.

2.2.7 Steenken, W. G., AIAA 88-3264, “Planar Wave Stability Margin Loss Methodology,” AIAA/ASME/SAE/ASEE 24th Joint Propulsion Conference, Boston, Massachusetts, July 11-13, 1988.

2.2.8 Reynolds, G. G., W. F. Vier and T. P. Collins, AFAPL-TF-73-43, “An Experimental Evaluation of Unsteady Flow Effects on an Axial Compressor-P3 Generator Program,” USAF AFAPL, July 1973.

2.2.9 Steenken, W. G., William, J. G., and Walsh, K. R., NASA/TM-1999-206587, “Inlet Flow Characteristics During Rapid Maneuvers for an F/A-18A Airplane,” October 1999.

2.2.10 Seybert, A. F. and C. U. R. Cheng, “Application of the Boundary Element Method to Acoustic Cavity Response and Muffler Analysis,” Journal of Vibration, Acoustics, Stress, and Reliability in Design, Vol. 109, pp. 15-21, January 1987.

2.2.11 Utsuno, H. and T. W. Wu and A. F. Seybert, “Prediction of Sound Fields in Cavities with Sound Absorbing Materials,” AIAA Journal, Vol. 28, No. 11, pp. 1870-1876, 1990.

2.2.12 Prakash, G. K. Ravi, “A Computational Method for the Analysis of Acoustic Radiation from Turbofan Inlets,” PhD dissertation under the direction of Dr. John Carruthers, University of Tennessee Space Institute, May 1992.

2.2.13 Peacock, R. E. and D. K. Das, “The Excitation of Compressor/Duct Systems”, Symposium on “Fluid/Structure Interactions in Turbomachinery,” Winter Annual Meeting of ASME, Washington, D.C., November 1-520, 1981.

2.3 Related Publications

The following publications are provided for information purposes only and are not a required part of this SAE Aerospace Technical Report.

2.3.1 Chung, K., Hosny, W. M. and W. G. Steenken, NASA CR-165141, “Aerodynamic Stability Analysis of NASA J85-13 Planar Pressure Pulse Generator Installation,” NASA, November 1980.

2.3.2 Das, D. K. and A. Trippi, AIAA-85-1135, “Effects of Inlet Pressure Fluctuations on Axial Flow Compressors: Some Experimental and Theoretical Results,” AIAA/SAE/ASME 21st Joint Propulsion Conference, July 1985.

2.3.3 Kimzey, W. F., AEDC-TR-77-80, “An Analysis of the Influence of Some External Disturbances on the Aerodynamic Stability of Turbine Engine Axial Flow Fans and Compressors,” August 1977.

2.3.4 Kuhlberg, J. F., D. E. Sheppard, E. O. King and J. R. Baker, AIAA 69-486, “Dynamic Simulation of Turbine Engine Compressors,” June 1969.

2.3.5 Lazalier, G. R. and J. T. Tate, AFAPL-TR-69-103, “Development of a Prototype Discrete Frequency, Total Pressure Fluctuation Generator for Jet Engine-Inlet Compatibility Investigations,” ARO Inc., AEDC, June 1970.

2.3.6 Mason, J. R., J. W. Park and R. F. Jaekel, NASA CR-165261, “Extended Frequency Turbofan Model,” December 1980.

2.3.7 McAulay, J. E., NASA TM X-2081, “Effect of Dynamic Pressure Variations in Engine-Inlet Pressure on the Compressor System of a Twin-Spool Turbofan Engine,” September 1970.

2.3.8 Milner, E. J., L. M. Wenzel and F. J. Paulovich, NASA TM X-3012, “Frequency Response of an Axial-Flow Compressor Exposed to Inlet Pressure Perturbations,” April 1974.

2.3.9 November, G., ASME Technical Paper 67-VIBR-57, “Causes of Variable Acoustic Resonance During Tests of Jet Engine Compressors,” 1967.

2.3.10 Peacock, R. E. and D. K. Das, “An Experimental Study of Pulsating Flow in a Three-Stage Axial Flow Compressor” Symposium on “Non-Steady Fluid Dynamics,” Winter Annual Meeting of ASME, San Francisco, CA, December 1978.

2.3.11 Peacock, R. E., D. C. Eralp and D. K. Das, AIAA 80-1080, “Compressor Response to Pulsed Transients,” AIAA/SAE/ASME 16th Joint Propulsion Conference, July 30-July 2, 1980, Hartford, CN.

2.3.12 Peacock, R. E. and D. K. Das, AIAA-81-1590, “Performance Analysis of a Family of Planar Pulse Generators,” AIAA/SAE/ASME 17th Joint Propulsion Conference, Colorado Springs, CO, July 27-29, 1981.

2.3.13 Steenken, W. G., AGARD Conference Proceedings No. 324, “Modeling Compression Component Stability Characteristics - Effects of Inlet Distortion and Fan Bypass Duct Disturbances,” AGARD Conference Proceedings No. 324, “Engine Handling,” Paper No. 24, October 1982.

2.3.14 Sussman, M. B. and G. W. Lampard, AFAFL-TR-69-103, “A Possible Mechanism for Inlet/Engine Interactions due to Inlet Flow Fluctuations,” 1969, Boeing Company, Commercial Airplane Division.

2.3.15 Wenzel, L. M., NASA TM X-1928, “Experimental Investigation of the Effects of Pulse Pressure Distortions Imposed on the Inlet of a Turbofan Engine,” November 1969.

2.3.16 Burcham, F. W. and Bellman, D. R., “A Flight Investigation of Steady-State and Dynamic Pressure Phenomena in the Air Inlets of Supersonic Aircraft,” Presented at the 38th Meeting of AGARD Propulsion and Energetics Panel, Sandeford, Norway, September 13-17, 1971.

2.3.17 McIlveen, M.W., AIAA 79-1185, “Further Test Results with the Airjet Distortion Generator System – A New Tool for Aircraft Turbine Engine Testing,” AIAA/SAE/ASME 15th Joint Propulsion Conference Las Vegas, NV, 1979.

2.3.18 Auzins, J., Society of Flight Test Engineers Journal, Vol. 2, “Measurement and Correlation of Structural Response to Inlet Hammershock Phenomena on an F-14 Airplane,” Grumman Aerospace Corporation, Calverton, New York, May 1980.

2.3.19 Billig, L. O., “Automatic Detection and Suppression of Inlet Buzz, Instruction for Air-Breathing Propulsion,” Proceedings of the Symposium, Monterey, CA, September 19-21, 1972, Boeing Company, Seattle, Washington.

2.3.20 Burcham, F. W. and P. G. Batterton, AIAA 76-653, “Flight Experience with a Digital Integrated Propulsion Control System on an F-111E Airplane,” NASA Flight Research Center, Edwards, CA, presented at AIAA/SAE 12th Propulsion Conference, July 1976.

2.3.21 Carter, E. G., AGARD-AR-81, “Technical Evaluation Report on Fluid Dynamics Panel Symposium on Airframe/Propulsion - A Discussion of Air Intakes, Nozzle Flow, and Flow Distribution,” AGARD Symposium at Rome, Italy, September 3-6, 1974.

2.3.22 Corbett, A. G. and Elder, R. L., “The Stability of Some Mathematical Models of an Axial-Flow Compressor,” University of Leicester - Rolls Royce Research Study, 1970-1972.

2.3.23 Corbett, A. G. and R. L. Elder, AGARD-CP-177, Paper No. 12, “Mathematical Modeling of Compressor Stability in Steady and Unsteady Flow Conditions,” September 1975.

2.3.24 Fraiser, H. R., Journal of Aerospace Sciences, “Supersonic Inlet Dynamics,” June 1960.

2.3.25 Gabriel, D. S., L. E. Wallner and R. J. Lubick, IAS Pre-Print 709, “Some Effects of Transients in Inlet Pressure and Temperature on Turbojet Engines,” Summarized in Aeronautical Engineering Review, January 1957.

2.3.26 Goethert, B. H. and W. F. Kimzey, 32nd Meeting of AGARD PEP, “Effect of High Frequency Fluctuations of Inlet Flow on Compressor Stall,” September 1968.

2.3.27 Goethert, B. H., AFAPL-TR-70-51, “Research and Engineering Studies and Analyses of Fan Engine Stall, Dynamic Interaction with Other Subsystem and System Performance,” July 1970.

2.3.28 Hercock, R. G. and Williams, D. D., AGARD Lecture Series 72, “Distortion Induced Engine Instability,” November 1974, Paper 3.

2.3.29 Kimzey, W. F. and S. H. Ellis, SAE Paper 740824, “Supersonic Inlet Simulator - A Tool for Simulation of Realistic Engine Entry Flow Conditions for F-15,” SAE National Aerospace Engineering and Manufacturing Meeting, San Diego, CA, October 1-3, 1974.

2.3.30 Kostin, L. C. and S. D. Millstone, AIAA 68-649, “Application of Statistical Parameters in Defining Inlet Airflow Dynamics,” June 1968.

2.3.31 Leynaert, J., FTD-ID (RSIT-1290-79), “Supersonic Air-Intake Buzz,” Presented at the 9th International Aeronautical Conference, Paris, June 2-4, 1969.

2.3.32 Lubick, R. J. and Wallner, L. E., “Stall Prediction in Gas Turbine Engines,” Journal of Basic Engineering, September 1959.

2.3.33 Martin, A. W. and W. D. Beaulieu, NASC CR-1631, “XB-70 Flight Test Data Comparisons with Simulation Predictions of Inlet Unstart and Buzz,” North American Rockwell Corporation, Los Angeles, CA, 1970.

2.3.34 Nagashima, T., T. Obokata and T. Asanuna, Institute of Space and Aeronautical Science Report No. 481, Vol. 37, “Experiment of Supersonic Air Intake Buzz,” Tokyo University, May 1972.

2.3.35 Newsome, R. W., AIAA 83-0175, “Numerical Simulation of Near-Critical and Unsteady Inlet Flow Fields,” AIAA 21st Aerospace Sciences Meeting, Reno, NV, January 10-13, 1983.

2.3.36 Schuerman, J. A., K. E. Fischer and P. W. McLaughlin, NASA CR 135313, “High Frequency Dynamic Engine Simulation,” July 1977.

2.3.37 Sugiyama, T., A. Hamed and W. Tabakoff, AIAA 78-246, “A Study on the Mechanism of Compressor Surge due to Inlet Pressure Disturbances,” January 1978.

2.3.38 Wasserbauer, J. F. and R. G. Willoh, AIAA Paper 68-651, “Experimental and Analytical Investigation of the Dynamic Response of a Supersonic Mixed Compression Inlet,” June 1968.

2.3.39 Weinreich, E. L., AGARD - “Ramjets and Ramrockets for Military Application, One-Dimensional Nonlinear Considerations on Supersonic Diffuser Buzz,” Messerschmitt-Boelkov-Blohm, Munich, AGARD Ramjets and Ramrockets for Military Application, 1982.

2.3.40 Weinreich, E. L., DR-ING Dissertation, “One-Dimensional Nonlinear Considerations Concerning the Stability Behavior of Inlet Diffusers for Supersonic Aircraft,” Darmstadt Technishe Hochschule, 1979.

2.4 List of Nomenclature and Symbols

TABLE 1

SYMBOL	TITLE	UNITS
AMP	One Half of Peak-to-Peak Planar Wave Pressure Fluctuation	psi
Ao/Ac	Inlet Mass Flow Ratio	-
AIP	Aerodynamic Interface Plane	-
C	Offset Coefficient	-
CR	Empirically Determined Factor Used to Relate ΔPRSPEAK and ΔPRSRMS	-
ECS	Environmental Control System	-
G	Gain	-
Hz	Frequency in Cycles per Second	sec^{-1}
IDC	Inlet Distortion, Circumferential	-
IDCMX	Inlet Distortion, Circumferential Maximum	-
IDR	Inlet Distortion, Radial	-
IDRH	Inlet Distortion, Radial at Fan Hub	-
IDRT	Inlet Distortion, Radial at Fan Tip	-
Kp(f)	Sensitivity of Compression Component to Planar Waves (ΔPRS/(ΔP/PIGV))	-
M	Mach number	-
NLR	Low Pressure Rotor Corrected Speed $N/\sqrt{\theta}$	rpm
(PAV)i	Ring i Average Total Pressure	psi
(PAVLOW)i	Circumferential Distortion Intensity Element for Ring i	psi
PFAV	Average Total Pressure at Fan Inlet	psi
Pi (t)	Time-Varying Total Pressure at the i-th of N probes	psi
PIGV	Total Pressure at Engine/Inlet Guide Vanes	psi
$\hat{P}(t)$	Time-varying Spatial-Average Total Pressure at the AIP	psi
P-P	Peak-to-Peak Pressure Differential	psi
PT0	Free-Stream Total Pressure	psi
PT1/PT0	Total Pressure Recovery at Measurement Plane	-
ΔP	Incremental Pressure	psi
PSD	Power Spectral Density $(PT0)^2/HZ$	$(psi)^2/Hz$
(ΔPC/P)i	Circumferential Distortion Intensity Element, Ring i	-
(ΔPR/P)i	Radial Distortion Intensity Element, Ring i	-
ΔPRS	Loss of Stability Pressure Ratio	-
S	Sensitivity, ΔPRS/(ΔP/PIGV)	-
W1R	Corrected Airflow at the Engine Face $W_1\sqrt{\theta}/\delta$	lb/s
α	Angle of Attack	deg
β	Angle of Sideslip	deg
δ	Ratio of pressure to standard reference pressure	-
Φ	Phase change from input to output	deg
ψ	Angle of Yaw	deg
ηr	Inlet total pressure recovery	-
$\eta(t)$	Time variant total pressure recovery at AIP	-
θ	Ratio of temperature to standard reference temperature	-
$(\theta^{-})i$	Circumferential Distortion Extent Element, Ring i	deg
$\Phi(f)$	Power Spectral Density Function	$(psi)^2/Hz$

3. SUMMARY

The subject of planar total-pressure waves has been reviewed to determine the feasibility of developing a consensus methodology that can account for the effect of planar waves on inlet/engine compatibility.

The review includes a problem assessment, a discussion of possible approaches to methodology definition, a description of testing requirements, conclusions, recommendations, and the results of a document review of planar wave material.

The problem assessment showed that planar waves have occurred at propulsion system operating conditions within normal flight envelopes during a number of aircraft development programs. Planar waves generally occur at low mass flow ratio and become more severe with increasing Mach number and decreasing airflow. Other sources, both internal and external, also can generate planar waves.

Planar waves often occur in combination with spatial total pressure distortion. The peak destabilizing event may not correspond to either a peak planar excursion or a peak spatial distortion. Because of the complex nature of the combined disturbance problem and the practice of exercising avoidance procedures, no well-developed consensus method exists for treatment of the combined planar wave/spatial distortion problem. This report defines an approach that is useful in methodology development.

A potential approach to methodology development is discussed which includes the following four key elements: (1) categorization of inlet planar waves, (2) determination of engine response to planar waves, (3) planar wave analysis methods, and (4) combined spatial total-pressure distortion and planar waves, including stability margin accounting. Elements of methodology validation are discussed in Appendix C.

Inlet and compression system component testing will be required to apply the proposed methodology to a specific system. Inlet testing is used to define the planar wave component at the AIP and compression system testing defines the response of the compression components to planar waves.

An assessment of the available data and published information from a document review identified some recent data that define the physical characteristics of planar waves. Several publications describe planar wave test techniques and compression system analytical models.

This report recommends that a well-planned analytical and experimental program be conducted to explore the sensitivities of turbine engines to planar waves in combination with various spatial distortion patterns.

4. INTRODUCTION

The information contained in this report represents the results from an effort to determine the feasibility of establishing and recommending a consensus methodology for identifying and assessing the effect of planar total-pressure waves on inlet/engine compatibility. It is intended to provide complementary guidance to the material provided for steady-state total-pressure distortion in References 2.1.1.1 and 2.1.1.2.

This effort was undertaken because it has been determined by engine tests and simulations that engine stability margin loss may occur due to one-dimensional, unsteady total-pressure fluctuations at the compressor face. These fluctuations are hereinafter referred to as planar waves and occur as in-phase total pressure oscillations. Reported sources of planar waves include both inlet-generated and externally-generated disturbances. The inlet-generated disturbances include separation, shock/boundary layer interaction, supersonic flight buzz/unstart, interaction with adjacent inlet/engines, instability during subsonic flight at low mass flow ratio, and supersonic inlet response to inlet control system inputs. Externally-generated total-pressure oscillations include vortex ingestion and ingestion of wakes from nose gear and/or bomb bay doors. Other external disturbances such as atmospheric gusts and explosions produce planar pressure ramps that are not oscillatory in nature. Explosions and armament firings have temperature ramps and/or spatial distortions associated with them. This document does not address either planar pressure ramps or temperature ramp/distortion effects. For an assessment of inlet/engine temperature ramp and distortion effects, the reader is referred to Reference 2.1.1.3.

Current recommended practices for handling engine inlet flow distortion do not account for the effects of planar waves on engine stability. Guidelines for handling planar waves and planar waves in combination with spatial total-pressure distortions are needed for inlet/engine systems.

This report assesses the planar wave problem through case histories and a discussion of combined spatial pressure distortion and planar pressure waves. It reviews techniques for categorizing inlet planar waves, reviews techniques for predicting engine response characteristics, presents an analysis methodology, and discusses the application of the methodology to combined planar waves and spatial pressure distortion. Validation of the methodology and testing requirements are also discussed. Finally, conclusions and recommendations are presented. Results of a review of documents related to planar waves are included in Appendix A.

The terms stability limit line, stability margin, and the loss of stability pressure ratio are used in this report to define impacts on the stability of a compression component. These terms are intended to represent, as appropriate or applicable, surge, stall, rotating stall, or other stability limits.

5. PROBLEM ASSESSMENT

In a number of aircraft development programs, planar waves have been detected by high-response pressure measurements at the aerodynamic interface plane (AIP). The planar waves have occurred at flight and propulsion system operational conditions within normal envelopes, i.e., their occurrence is not restricted to extreme corners of the flight or maneuver envelopes. Tests and computer simulations of compressors and engines with planar waves have indicated that engine stability can be adversely affected by these waves, depending on the frequency and amplitude of the disturbance.

Trends in aircraft design that may impact planar wave generation include:

- Increased use of internal bays for weapons carriage and the need to have full envelope weapons capability, resulting in increased risk of wake ingestion when they are open.
- Aircraft post-stall maneuvering capabilities, which could lead to conflicts between flow dynamic boundaries and aircraft maneuvering requirements not previously encountered in traditional designs.
- Active control of the engine stability margin for performance optimization. This reduces available stability margin in parts of the flight envelope, compared to prior stability margin design criteria.
- Minimizing the inlet/engine airflow for “supersonic lock-up" to improve aircraft deceleration characteristics from high Mach number conditions.
- Low observables features in the air induction system.

With these items increasing the probability of encountering inlet planar waves, there is reason to believe that future designs are at increased risk. Therefore, it was considered necessary to determine whether a methodology could be established to predict the effect of planar waves on stability margin, in order to ensure continued inlet/engine compatibility.

To assess the planar wave problem, case histories where planar waves occurred were examined and the problems of analyzing combined planar waves and spatial total pressure distortion were investigated. The results from these studies are presented in Sections 5.1 and 5.2.

5.1 Case History Studies

Two recent case histories were selected as examples of situations in which planar waves have occurred. These cases illustrate some of the causes of planar waves, provide examples of instrumentation used to detect and measure planar waves, and indicate the extent of configuration and operational changes accomplished to eliminate or reduce the magnitude of the planar wave problem.

5.1.1 System “A”

During the wind tunnel and flight test development program of System “A,” several sources of planar waves were encountered. These sources included: (1) inlet duct resonance at low engine power settings and therefore low mass flow ratios, (2) Environmental Control System (ECS) precooler duct resonance and (3) nose gear wake ingestion. Details of these data are presented in Reference 2.2.1.

5.1.1.1 Inlet Duct Resonance

It was found that one source of low mass flow ratio planar waves is local flow separation and re-attachment along the vertical ramp surface forward of the cowl during leeward sideslip as shown in Figure 1. This separation is due to a highly adverse pressure gradient forward of the cowl lip station interacting with the boundary layer along the forward ramp surface. As leeward sideslip increases, the flow expands around the ramp leading edge, and then decelerates rapidly to the inlet station. Local ramp pressures decrease near the leading edge which allow boundary layer thickness to increase prior to entering the high-pressure-gradient region. The process is similar, although at much lower amplitudes, to buzz at supersonic speeds caused by shock wave and boundary layer interactions. Horizontal ramp inlets experience this phenomenon at low or negative angles of attack; vertical ramp inlets experience this phenomenon at leeward sideslip.

Representative wind tunnel and flight test distortion characteristics measured at Mach 0.85 are presented in Figure 2. Power spectral densities identify the presence of discrete frequency components with a fundamental frequency of 60 Hz (0.2-scale; 12 Hz full scale). This frequency corresponds well with open-closed end organ pipe theory, calculated as

$$f = c/[4(L+X)]$$

where:

c = speed of sound

f = first fundamental frequency of the duct

L = duct length from cowl lip to the reflection plane represented by the engine

X = organ pipe end correction (sometimes set to 1.4 x effective diameter of duct)

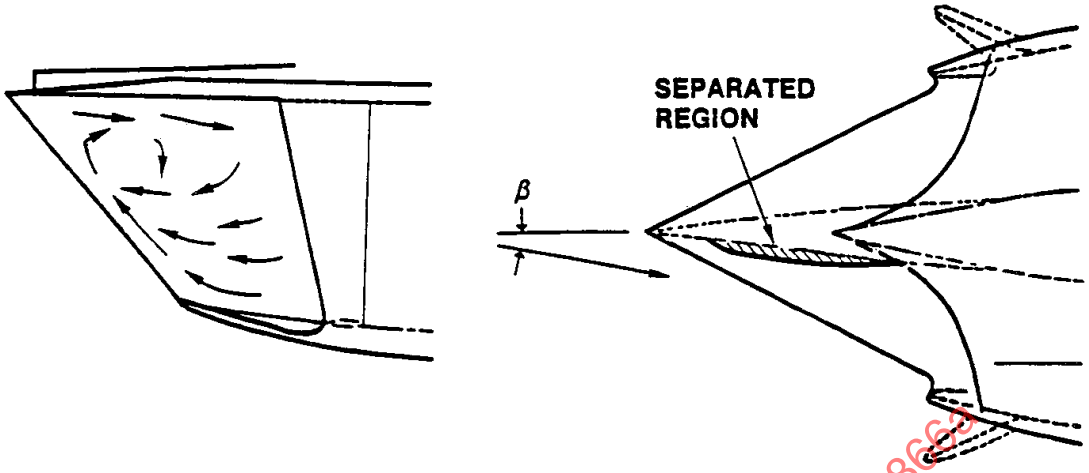

FIGURE 1 - LOCAL FLOW SEPARATION ON INLET RAMP DURING OFF DESIGN OPERATION AT LOW AIRFLOW

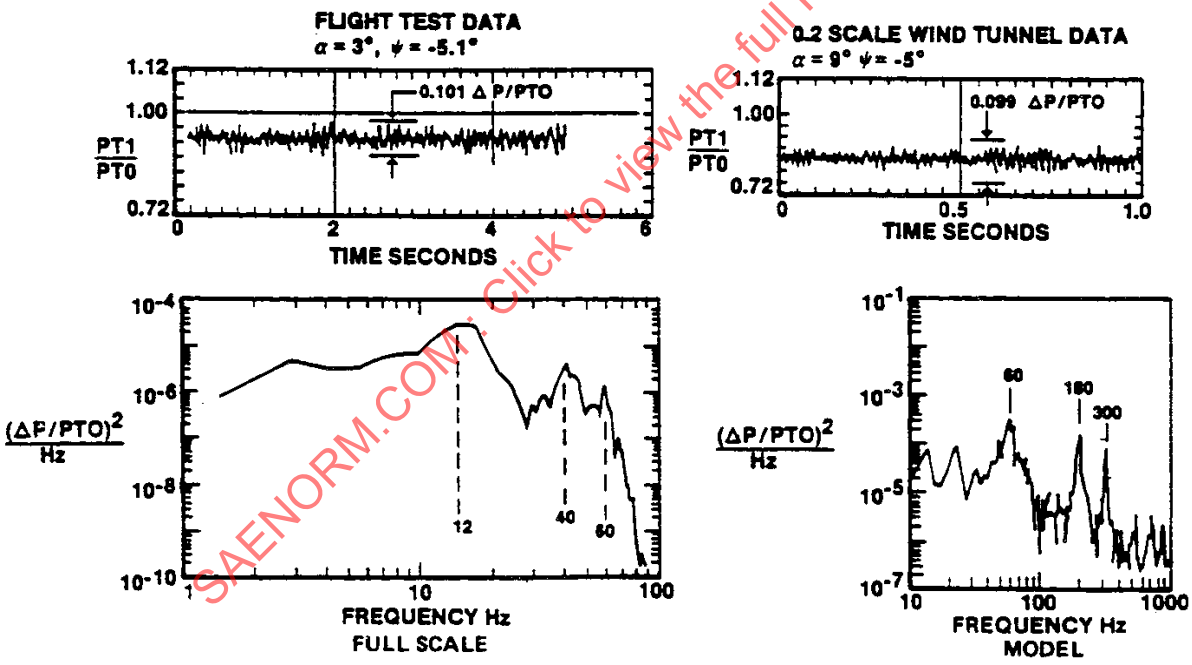

FIGURE 2 - WIND TUNNEL/FLIGHT TEST COMPARISON OF PLANAR WAVES, MACH 0.85

Magnitudes of the planar waves are strong functions of geometry, corrected airflow, attitude and Mach number. Examples of some of these factors are shown in Figure 3. The planar wave effect increases with increased Mach number and decreased flow. The peak-to-peak amplitudes of the planar waves can become quite large (e.g., 16 to 20% of mean total pressure). Representative total-pressure spatial-distortion characteristics are presented in Figure 4 as specific distortion indices. Circumferential distortion is the predominant spatial component, although both components increase almost proportionately with corrected airflow. Flight test results generally confirm wind tunnel results.

There were no discernible effects on stability due to the planar waves. A manually operated idle speed lock-up feature was incorporated to increase the minimum airflow and thereby reduce the amplitude of the planar wave.

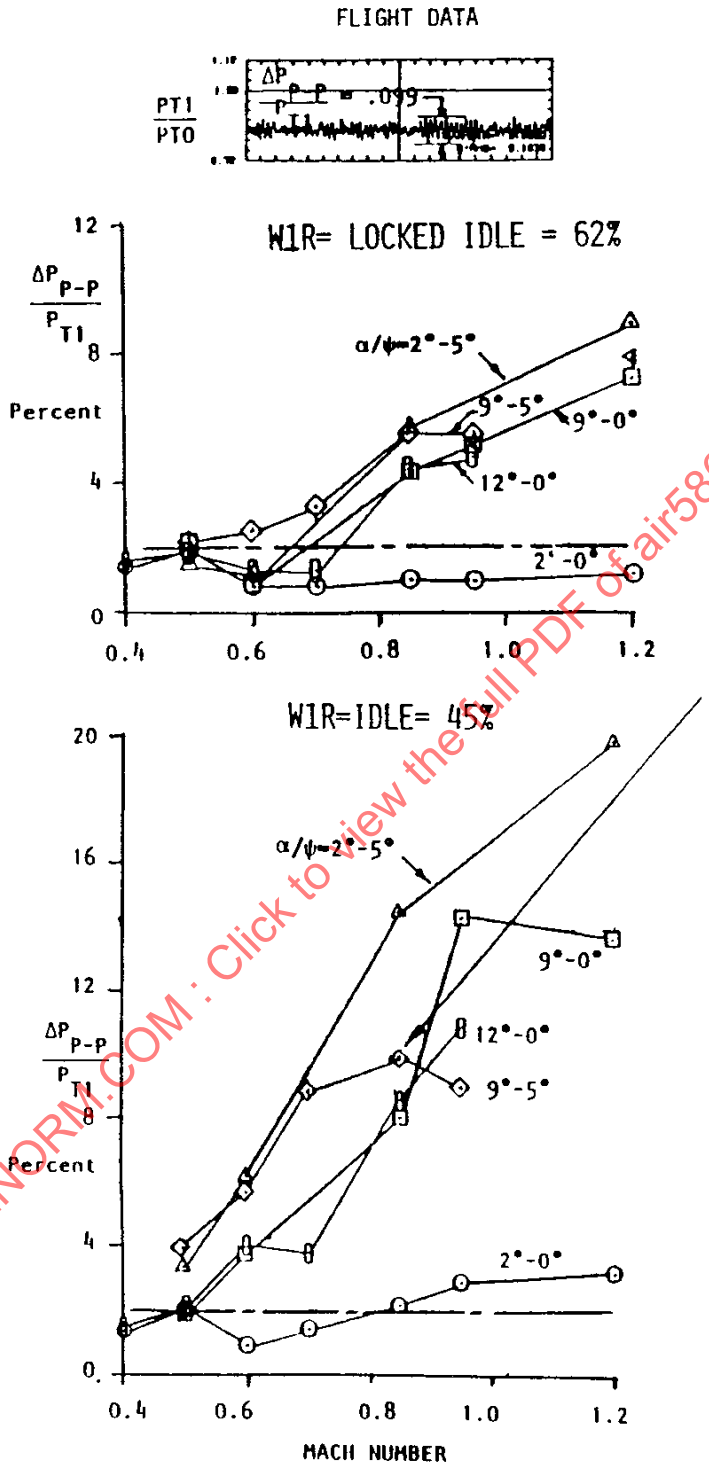

FIGURE 3 - PLANAR WAVE AMPLITUDE

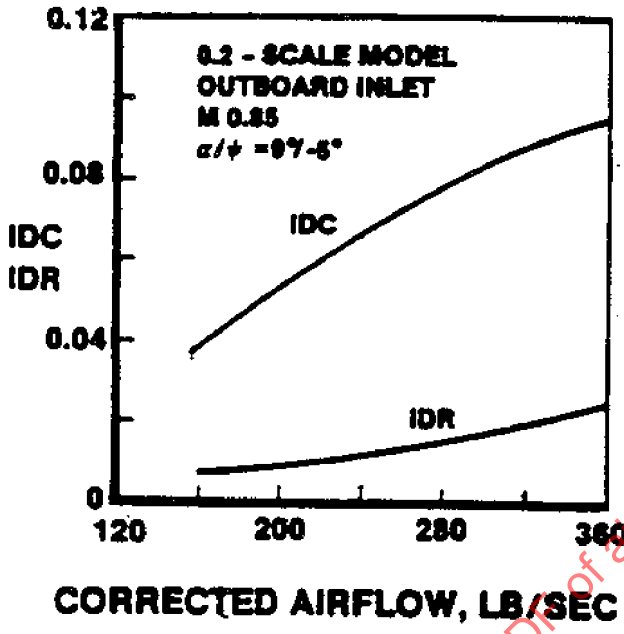

FIGURE 4 - SPATIAL DISTORTION CHARACTERISTICS

5.1.1.2 Inlet Precooler Resonance

Auxiliary air inlets were also found to be a source of internally generated disturbances. A scoop installed on the ramp side of each inlet to precool ECS bleed air (Figure 5) acted as a resonator (open-closed organ pipe). The resulting pressure disturbance propagated to the AIP. High-response pressure transducers located just upstream of the flapper door in the aircraft identified duct resonance at frequencies corresponding to an open-closed organ pipe. During static operation at maximum engine airflow, power spectral densities (Figure 6) identified a fundamental frequency at 77 Hz (full-scale) as well as the presence of several harmonics. RMS amplitudes were approximately 2.4 psi. Because of the design of the original ECS air scoop, resonance could lead to structural damage. The flapper door was redesigned to eliminate the problem.

5.1.1.3 Nose Gear Wake Ingestion

Nose gear wake ingestion was found to be a source of externally generated disturbances. System “A” flight test investigations showed that the nose gear produced planar waves (Figure 7). Peak-to-peak amplitudes of the engine-face average total pressure were approximately seven percent of the mean total pressure. The fundamental frequency was 18 Hz (full-scale) at Mach 0.40 increasing to 28 Hz at Mach 0.60. A three-position cowl lip was incorporated into the System “A” design which makes it possible to place the lip in a position that minimizes the effect of the landing gear wake ingestion. In this position, the disturbances caused no discernable impact on engine stability.

5.1.2 System “B”

During the flight test program of System “B” aircraft, planar waves were recorded at a number of flight conditions (Figure 8) when the engine was operating at idle and below idle airflows during engine airstarts. These planar waves had a peak-to-peak pressure fluctuation amplitude of as much as 20% and occurred at a frequency of 11 Hz at sub-idle airflow. A data trace showing typical planar waveforms from the high-response data as well as a data trace showing the pressure fluctuations measured without the presence of planar waves are presented in Figure 9.

An analysis of the engine and inlet operating conditions at the times the planar waves occurred (Figure 10) shows that the planar waves occurred at idle and below idle airflows. Also presented in Figure 10 are the conditions where planar waves occurred as a function of inlet mass flow ratio, illustrating again the low airflow conditions under which the planar waves have occurred. The data show that these planar waves occur at low mass flow ratio and become more severe with increasing Mach number and decreasing airflow.

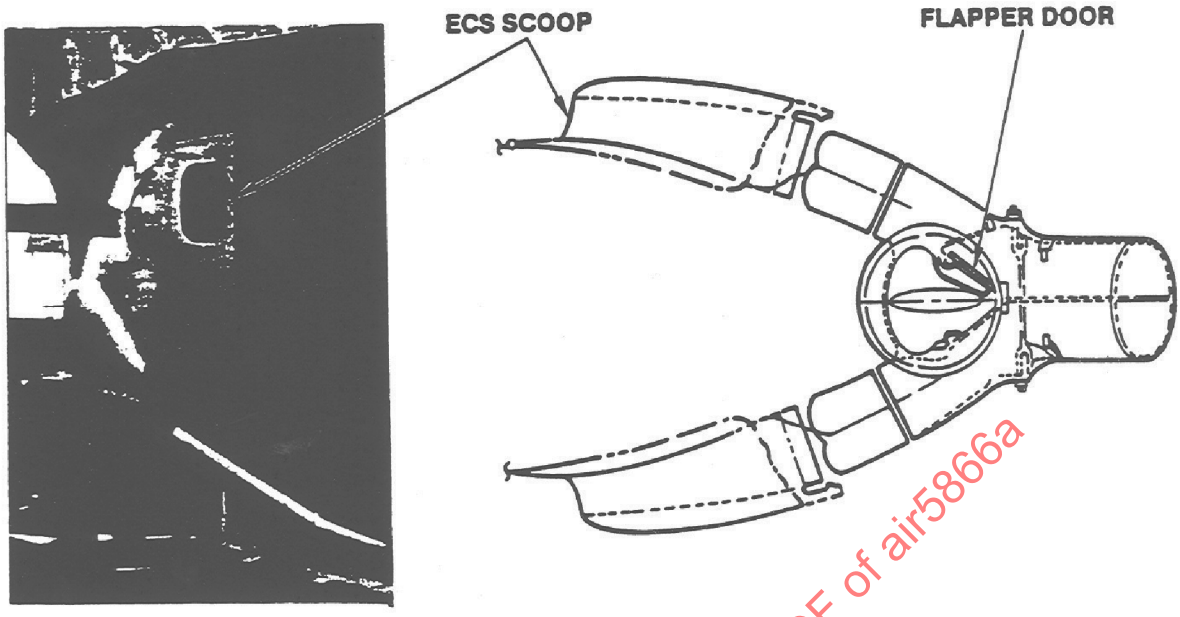

FIGURE 5 - ECS PRECOOLER ASSEMBLY

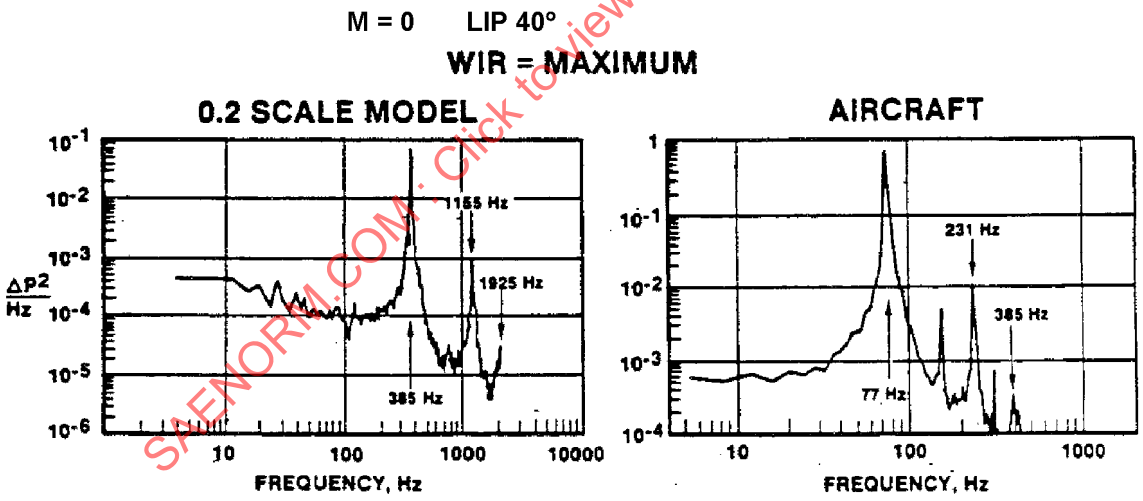

FIGURE 6 - RESONANCE CHARACTERISTICS IN ECS SCOOP INLET

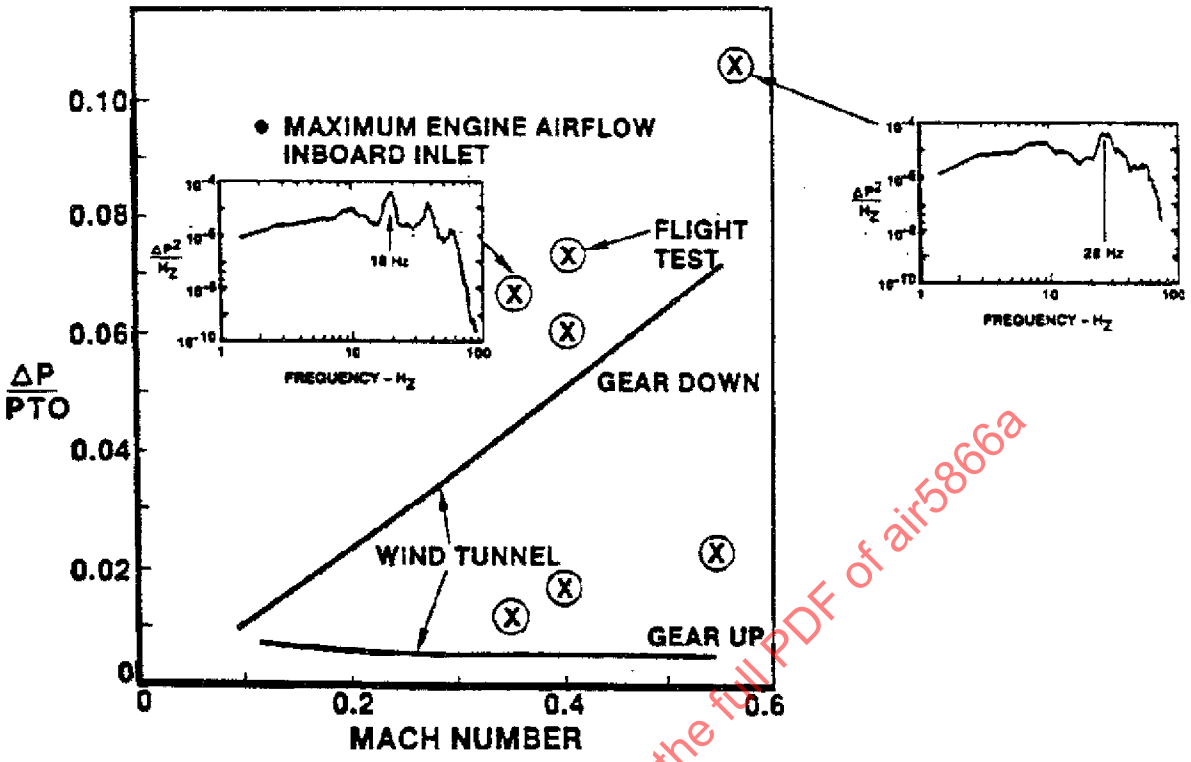

FIGURE 7 - EFFECT OF GEAR WAKE INGESTION ON PLANAR WAVES

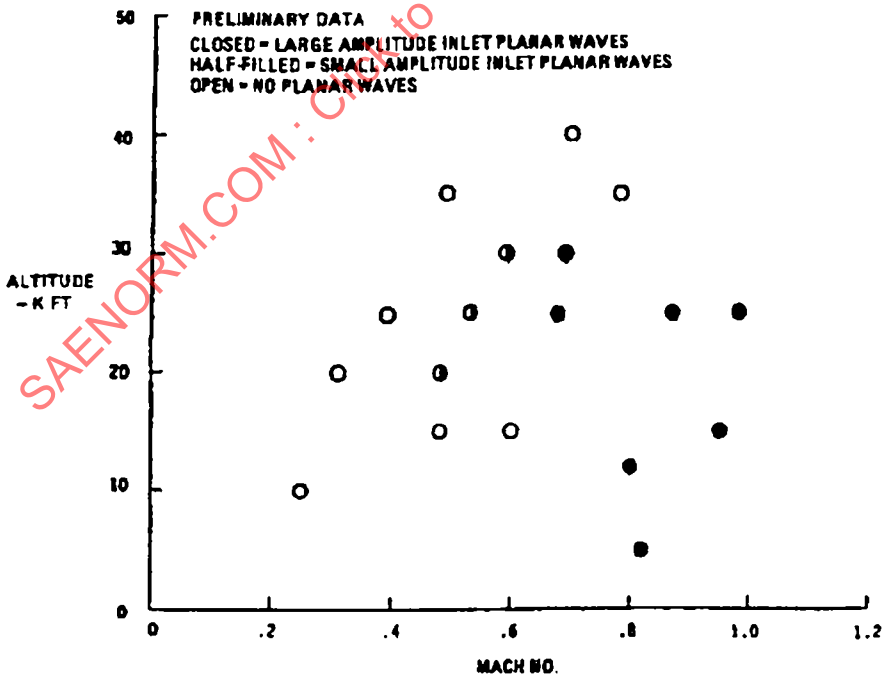

FIGURE 8 - COMPRESSOR INLET PLANAR WAVE EXPERIENCE AS A FUNCTION OF FLIGHT PROFILE FOR IDLE AND BELOW IDLE AIRFLOWS

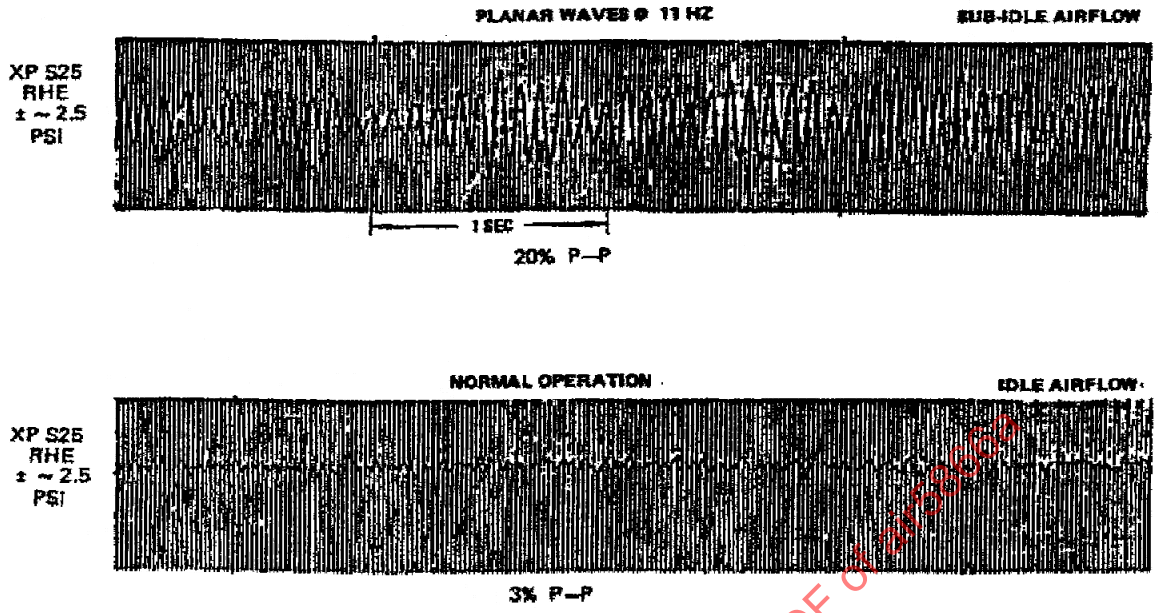

FIGURE 9 - COMPRESSOR INLET PRESSURE SIGNATURES

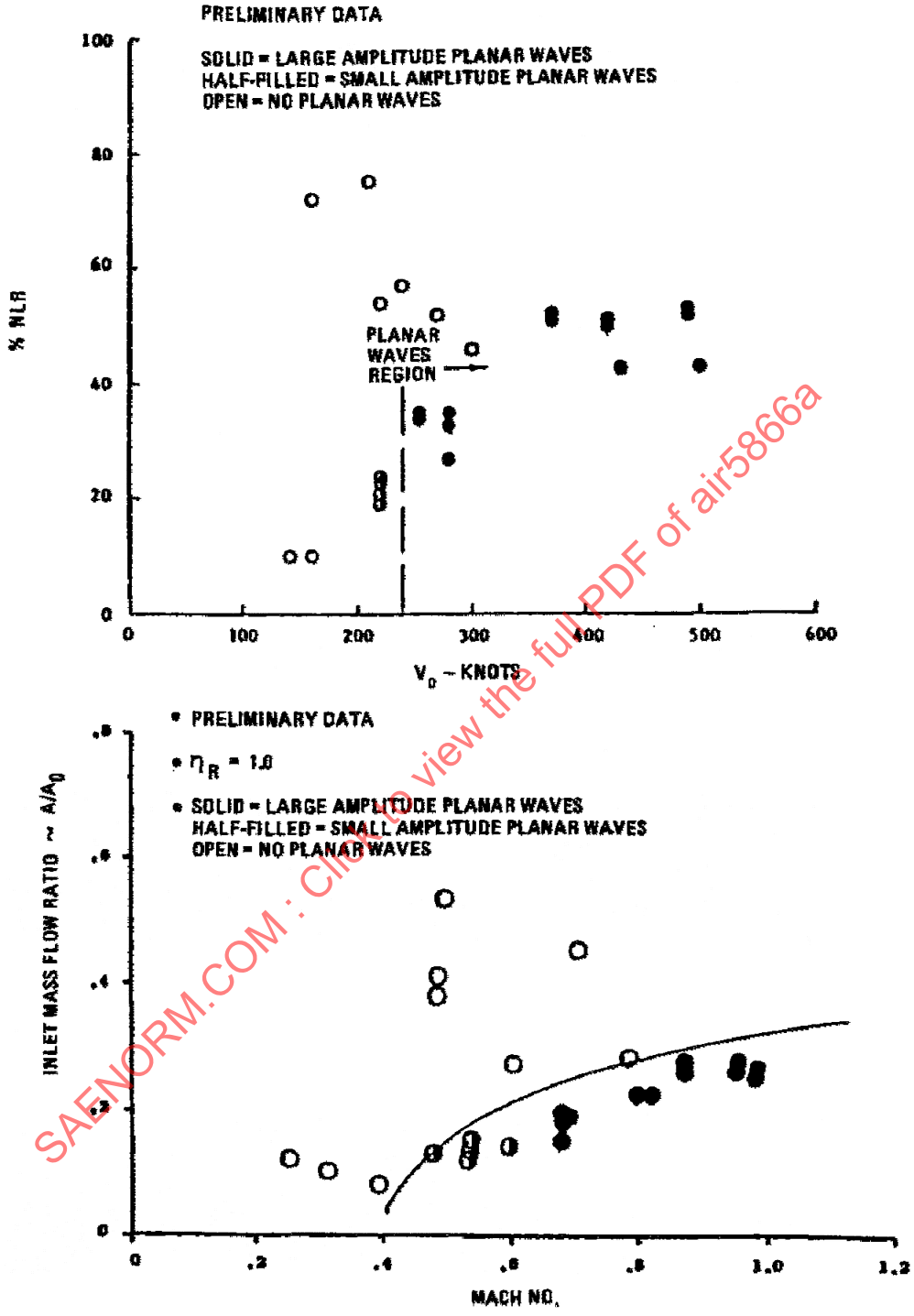

FIGURE 10 - COMPRESSOR INLET PLANAR WAVE EXPERIENCE AS A FUNCTION OF ENGINE SPEED AND INLET MASS FLOW RATIO

During development of System “B” aircraft, 1/7-scale wind tunnel model high-response data were measured. These data were analyzed to provide the compressor face waveform and total-pressure contour plots for idle airflow conditions at Mach 0.90 and 0.75. Some of these data for Mach 0.90 are presented in Figure 11 to illustrate typical planar waveforms and spatial distortion parameters. These distortion parameters were generated with procedures similar to those defined in ARP1420 (Reference 2.1.1.1). Power spectral density (PSD) plots of the waveforms and spatial distortion factors are presented in Figure 12. These PSDs identify a fundamental frequency of 50 Hz (model scale) as well as several harmonic frequencies.

From the results of the flight test experience of System “B,” it can be inferred that the potential exists for heavy pressure fluctuations at airspeeds above 240 knots during air starts. The impact of these pressure fluctuations on engine starting, however, is undefined. During the flight test program, no engine instabilities were observed during operation with planar waves at idle power setting and above.

5.2 Combined Spatial Pressure Distortion and Planar Waves

Spatial time-variant total pressure distortion induced at the AIP by inlet turbulence is random in nature and is accompanied by random variations in face-average total pressure. An example illustrating the variation of inlet recovery factor accompanying the variation in a typical spatial-distortion-descriptor is presented in Figure 13. For most applications, the planar wave contribution is small and may be neglected. Thus, the spatial distortion elements and descriptors formulated in ARP1420 (Reference 2.1.1.1) and AIR1419 (Reference 2.1.1.2) do not distinguish between time-variant and steady-state face-average total pressure.

As indicated in Section 7 of Reference 2.1.1.2 and discussed earlier in this report, shock/boundary layer interactions in supersonic inlets can give rise to distortion with a high planar wave or “in-phase” pressure component.

Data taken from System “B” (3.1.2) present a further example. The planar waves can take various forms and be either cyclic or random in time. Where the planar-wave amplitude begins to become significant (on the order of 1% of steady-state face-average pressure), the need for a methodology to account for the combined effects of spatial and planar distortion on engine stability margin should be considered as part of inlet/engine compatibility assessment.

One approach is provided by Burstadt and Wenzel (Reference 2.2.2). The possible accounting methods are discussed in Section 6, but it is worth mentioning here that all methods require quantification of the intensities of the planar-wave and spatial distortion elements in a combinatorial algebra that takes into account their time phasing. The peak destabilizing event may correspond to neither a peak planar nor a peak spatial distortion.

As a result of the inlet/engine design practice to avoid planar waves, a well-developed method for the treatment of the combined disturbance has not been developed. Thus, while the problem is theoretically tractable and appears straightforward computationally, little or no direct validation data for multispool engines exist, at least in a systematic codification. This report presents a methodology for assessing the effects of combined spatial total-pressure distortion and planar waves on compression system stability.

6. APPROACH TO PLANAR WAVE METHODOLOGY

In developing the proposed planar wave stability methodology, one of the primary ground rules has been to retain the stability accounting approach used in ARP1420. That is, the definitions and measurements needed to evaluate time-variant spatial distortion should not be required to change. Stability margin accounting should continue to be implemented at constant corrected engine airflow.

In addition, a methodology to account for the effects of planar waves on engine stability should include the following three elements: (1) categorization of the planar waves produced by the inlet and upstream systems and the flight conditions at which they can be expected to occur, (2) determination of the engine response to the types of planar waves that can be expected, and (3) a prediction methodology that relates the measured inlet pressure oscillations and the engine response characteristics to a loss of stability margin. The above three elements are presented in this section of the document. Methodologies for combining planar wave effects and spatial total-pressure distortion are also presented.

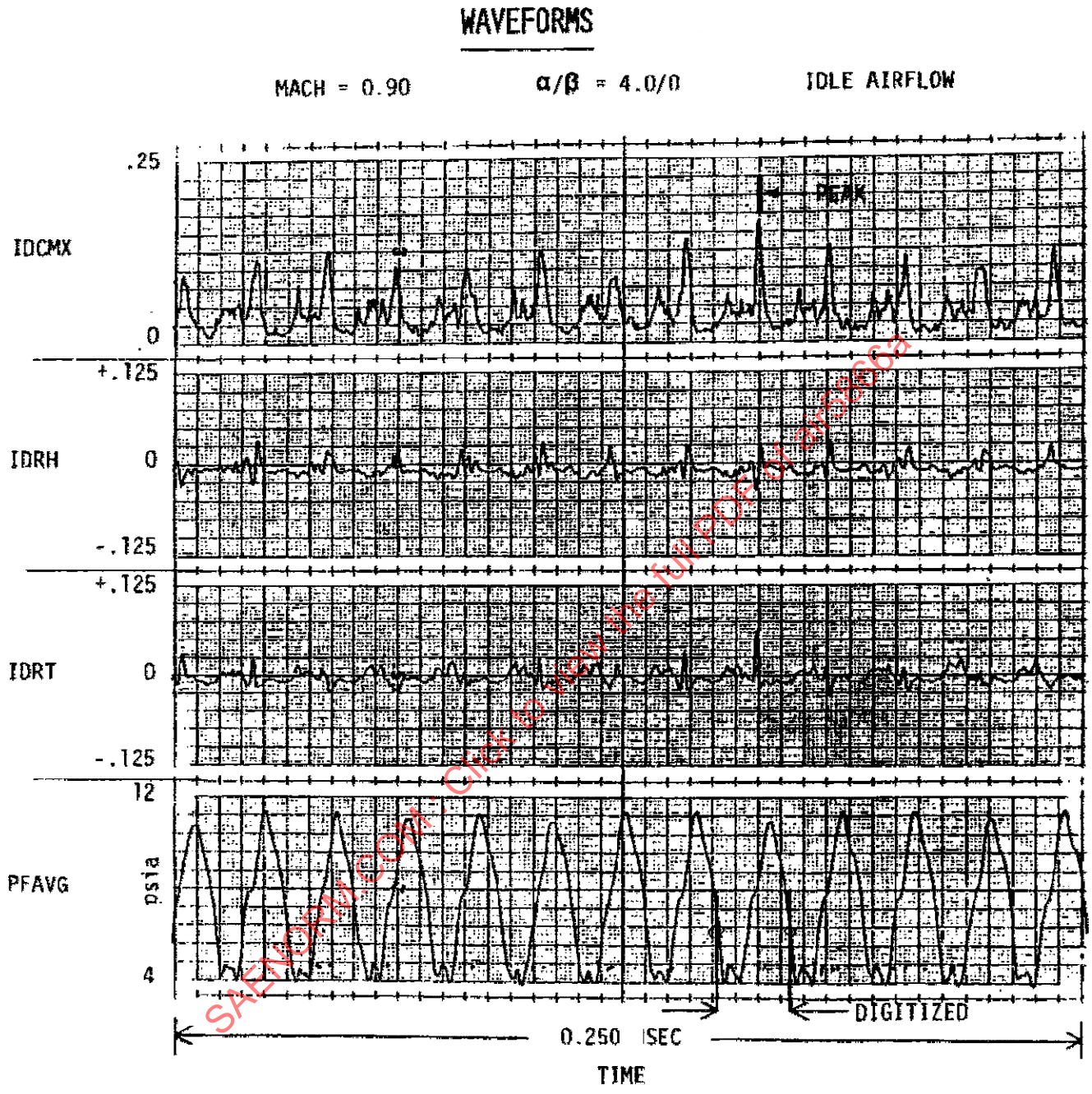

FIGURE 11 - WAVEFORMS OF COMPRESSOR FACE AVERAGE TOTAL PRESSURE AND DISTORTION FACTORS

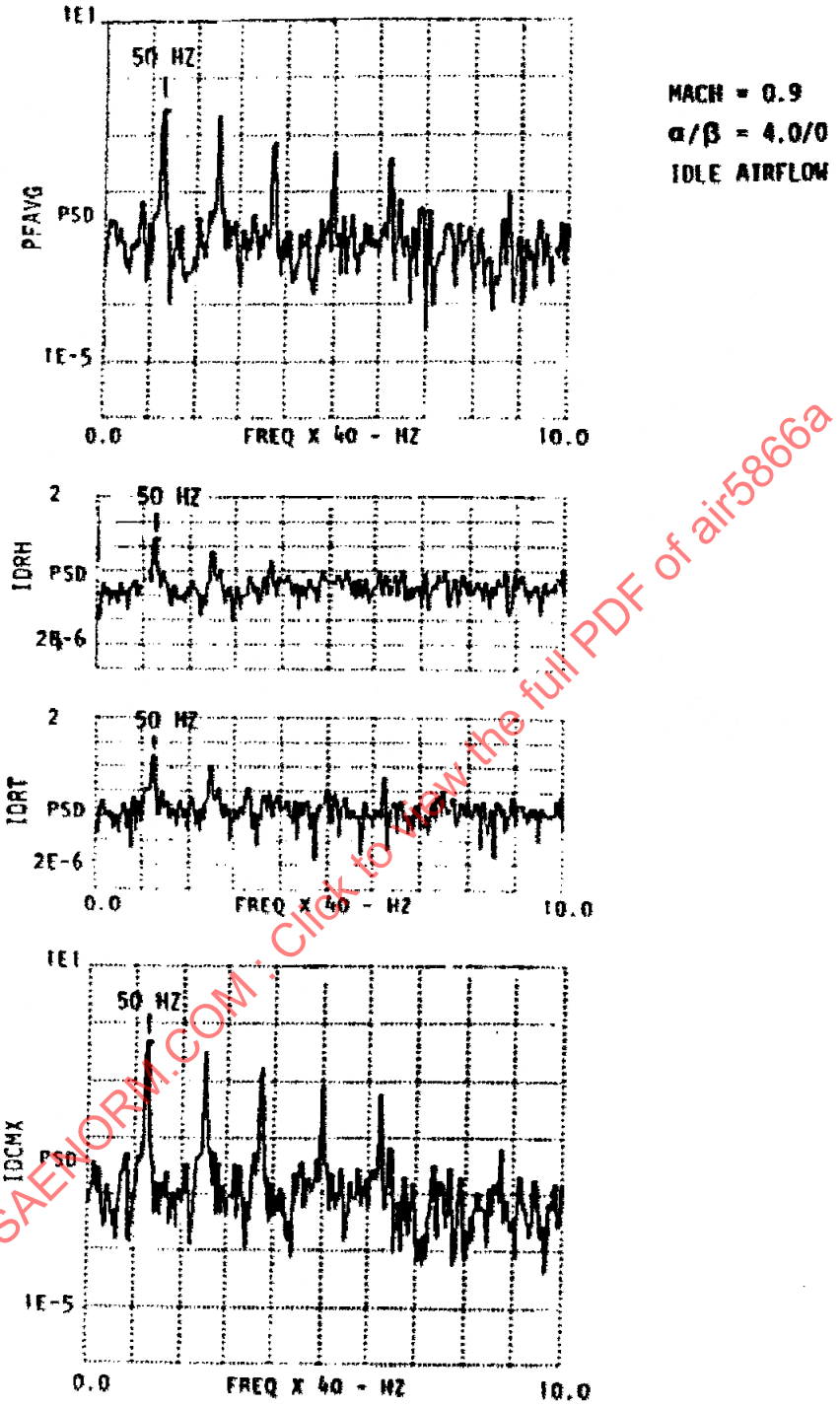

FIGURE 12 - POWER SPECTRAL DENSITY PLOTS OF WAVEFORMS

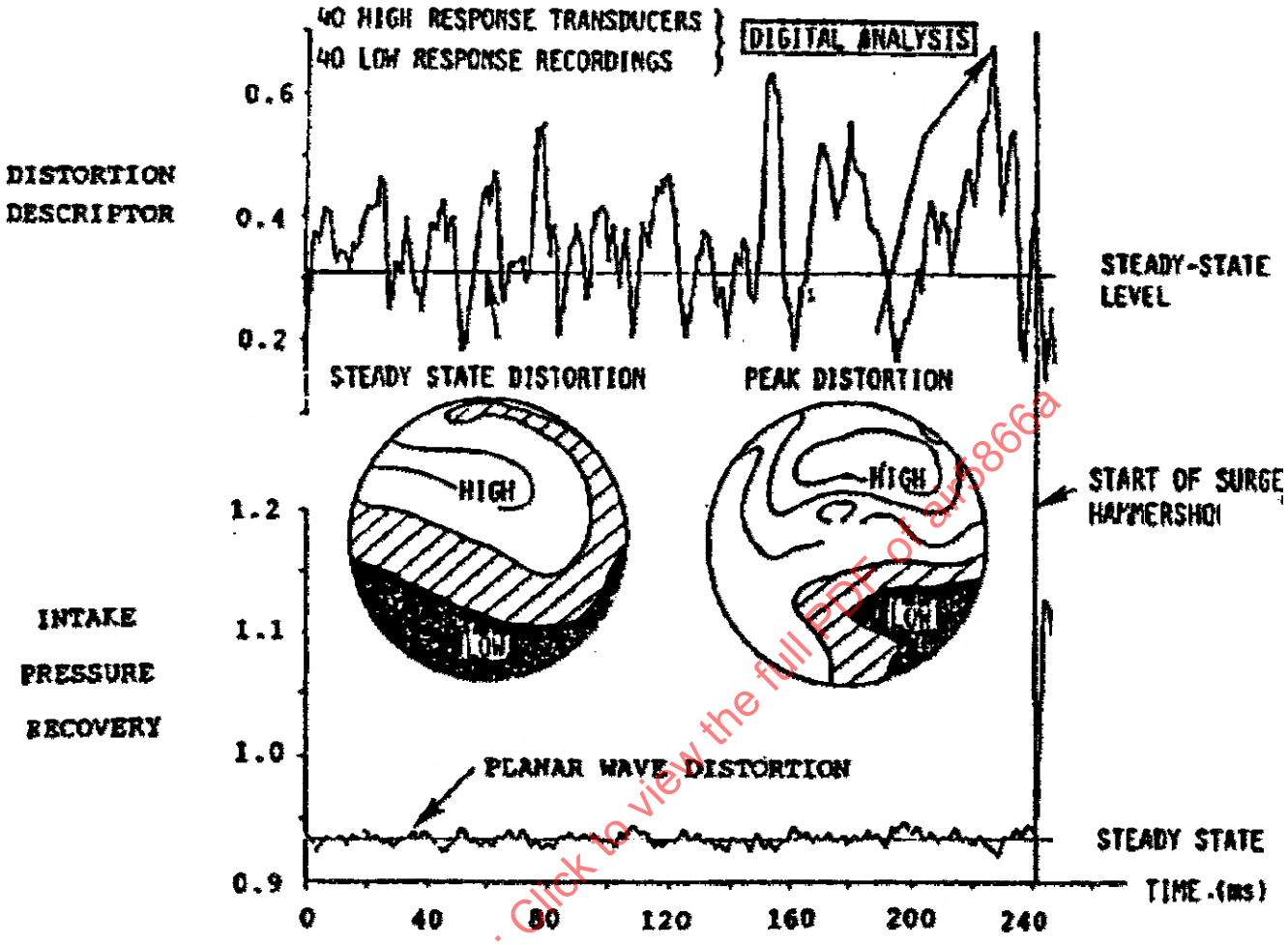

FIGURE 13 - TIME-VARIANT DISTORTION, INLET PLUS ENGINE TESTS

6.1 Categorization of Inlet Planar Waves

Planar waves can be categorized through use of the power spectral density (PSD) of the time-varying compressor-face-average total-pressure recovery. That is, planar waves are defined for the N probes of an inlet AIP rake-probe array as follows:

$$\hat{P}(t) = \frac{1}{N}\sum_{i=1}^{N} P_i(t) \qquad \text{(Eq. 1)}$$

where:

$P_i(t)$ = time-varying total pressure at the i-th of N probes

$\hat{P}(t)$ = time-varying spatial-average total pressure at the AIP

The various types of planar waves commonly encountered are summarized in Figure 14. Periodic variations such as short-duration ramps may also occur, e.g., as a result of supersonic intake compression surface movement. Four categories of inlet data are identified, and illustrated as time-trace and power-spectral-density (PSD) data. Typical distortion sources are shown. The amplitude and frequency content of the planar wave distortion depends on the severity of the disturbance and intake scale. Buzz frequencies are typically on the order of 20 Hz or less at full scale.

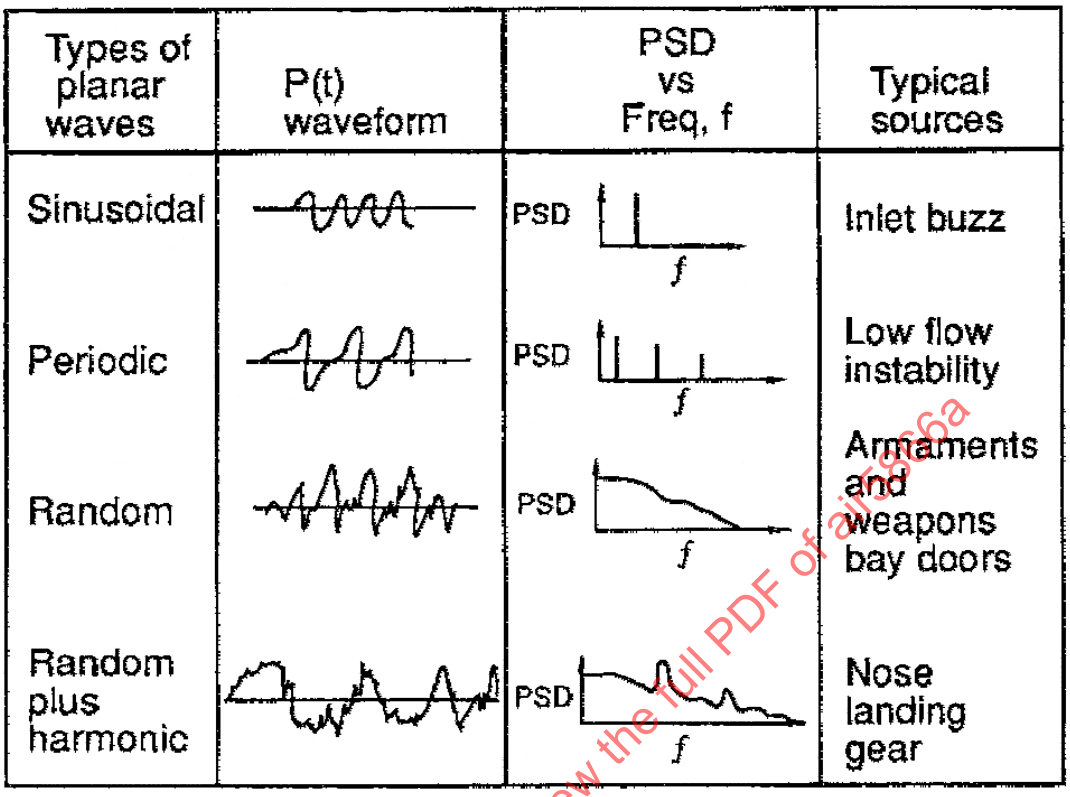

FIGURE 14 - CATEGORIZATION OF INLET DATA

Periodic waves are deterministic planar waves that have a finite number of constituent frequencies and can be broken down into their constituent harmonics by Fourier analysis. They can then be described as the summations of series of sine waves each of amplitude, $P(t)_n$, circular frequency, (n), and phase, ϕ (n):

$$\hat{P}(t) = \bar{P}(t) + \sum_n \left[\hat{P}(t)_n \bullet \mathrm{Sin}(\omega_n t + \phi_n)\right] \quad \text{(Eq. 2)}$$

The power spectral density of periodic waves consists of numbers of discrete spikes at each frequency with, ideally, no background noise. Conceptually, the harmonics of the periodic waves can be analyzed using compression-component distortion sensitivities established for discrete-frequency disturbances and the resulting n values of ΔPRS added appropriately to yield an overall ΔPRS. The additions are not straightforward as superposition considerations involving the phase relationships between the wave components have to be taken into account.

Early categorization of the type of planar wave to which an engine is being subjected is helpful in establishing the degree of sophistication needed to estimate the loss of stability margin due to inlet planar waves. This will be discussed later in this section. It is important to examine all the frequencies with high power levels since the total effect of all harmonics may cause a greater loss of stability pressure ratio (ΔPRS) than the fundamental frequency. For the purposes of calculating a planar waveform as in Equation 1, current practice would dictate using inlet probe data with the same frequency response as is used for the time-varying spatial distortion calculations, that is, data typically low-pass filtered to one rotor revolution (Reference 2.1.1.1).

6.2 Determination of Engine Response to Planar Waves

Considerable care must be exercised in generating stability results obtained from vehicles tested with planar pressure waves. As will be discussed, a typical method for the presentation of sensitivity to planar waves is to formulate the ratio of the loss of stability pressure ratio (based on the average operating point of a compression component at instability) to the amplitude of the planar wave at a given frequency. This formulation is similar to defining spatial distortion sensitivities and defines a sensitivity that requires that the wave content at the given frequency be purely sinusoidal.

Further, the inlet waveform depends importantly on the inlet and exit duct lengths and the placement of the flow-measuring plane relative to the engine face, for the standing wave that acts as an acoustic reflection plane in the vehicle installation. As previously mentioned, the standing-wave structure plays an integral part in determining the planar wave amplitude.

Another important role of test data is to validate computer simulations. If one can obtain the same result with a computer simulation of the test vehicle as is obtained from test, then one would expect that a valid result would be obtained with the same compression component operating in a different geometrical configuration. Alternatively, the employment of the validated computer simulation with a new compression component in a new geometrical configuration would yield an equally valid result.

6.2.1 Engine or Compression System Tests

Experimental definition of system responses to planar waves is the preferred approach. Discussion of requirements/guidelines is deferred to Section 7 where they are presented in detail.

6.2.2 Computer Simulations

Determination of engine responses to inlet-generated planar waves requires using appropriate engine and compression-component computer models that have been validated by comparison with test data. Such models use numerical methods that solve lumped or distributed forms of the one-dimensional unsteady-flow mass, momentum and energy conservation equations, with allowance for radial flows in the bypass splitter region for turbofan engines. Fans and compressors may be modeled using overall, stage, or row performance characteristics depending on the frequencies of interest. They may be assumed to operate quasi-steadily provided the upper frequency of interest is not too great. When constructing such models, it is important to decide upon the frequency range relevant to the application. The upper limit of the frequency range can be used to determine the maximum lumped-volume length that can be used and still give the desired fidelity. Once this choice has been made, then the compression component can be appropriately represented. Some of the major considerations that must be taken into account when putting together a computer simulation are itemized in Figure 15. The types of models that might be employed are listed in order of increasing sophistication and concomitantly increasing frequency capability.

For low frequency disturbances in the range up to approximately 5 Hz, a standard engine transient model may be used. As the frequency range increases, gas-path volume dynamics become increasingly important and need to be accounted for, initially on a compression-component basis (with appropriate duct volume assignments), then progressively by modeling on a stage-group basis (Reference 2.2.3), a stage-by-stage basis (Reference 2.3.4) and, ultimately a blade row basis (References 2.2.5 and 2.2.6). Current inlet problems have not required a model of higher order than a stage-by-stage model. Overall compression system models operate up to approximately 30 Hz and cover most inlet problems of interest.

In addition to the loss of compression system stability by direct aerodynamic effects, the engine might respond to planar waves through its control system via sensors in the gas path that could result in transient changes in fuel flow. The total effect on the engine will be governed by the response (amplitude and phase) of individual components of the control and fuel systems, e.g., transducer sensitivity, tubing lengths from the sensor head, control logic, fuel pump, etc. Fuel control during transients may be affected, for example, through any pressure-ratio limiter.

- TYPE OF MODEL IN ORDER OF INCREASING FREQUENCY CAPABILITY
  - STANDARD TRANSIENT MODE (0-5 HZ)
    (RIGID ROTOR DYNAMICS ONLY)
  - TRANSIENT MODEL WITH VOLUME DYNAMICS
    - ✓ COMPRESSION COMPONENT LUMPED INTO ONE VOLUME (0 – 20 HZ)
    - ✓ COMPRESSION COMPONENTS LUMPED INTO BLOCKS OR STAGES (0 – 50 HZ)
    - ✓ STAGE BY STAGE (0 – 150 HZ)
    - ✓ BLADE ROW BY BLADE ROW (0 – 250 HZ)
- ENGINE CONTROL / RESPONSE
- GAS PATH SENSORS / RESPONSE
- VARIABLE GEOMETRY ACTUATORS / RESPONSE

FIGURE 15 - ENGINE AND COMPRESSION SYSTEM COMPUTER SIMULATION CONSIDERATIONS

A typical time constant for engine response to control system input step changes may be approximately 200 ms, implying a time delay approaching 600 ms to achieve 99.6% of the total change. In this case, no significant response to cyclic planar waves with frequencies greater than 5 Hz would be expected. Engine experience to date (with large engines) indicates little measurable change in engine parameters with control system inputs of high planar-wave amplitudes of approximately 25% at frequencies greater than 3 Hz.

Because of the complexity and cost associated with determining engine-test planar-wave sensitivities, computer simulations are playing an increasingly important role in describing the response of an engine to planar waves.

6.2.3 Analytical Solutions

In some situations, the planar wave analysis problem can be simplified. This simplification can stem from the frequency range of interest, a desire to obtain trend information, and/or to provide physical insight into the problem.

At low planar-wave frequencies, in the range up to approximately 30 Hz, the wavelengths of the total-pressure disturbances are large in relation to the length of a fan or compressor. These components can be regarded as operating quasi-steadily on an overall basis. A considerable simplification results when the instantaneous pressure ratio of the fan or compressor and hence, its stability margin utilizations, can be computed from the phase relationships across the component. A simple semi-analytical expression may be formulated using the magnitude of the phase-change relationship established numerically from lumped-volume or distributed-volume gas dynamics models.

An analytical model for estimating compressor sensitivity to a sinusoidal total-pressure planar wave is presented in Appendix B. The compressor instantaneous pressure ratio is formulated in terms of inlet and outlet total-pressures and the gain, G, and phase, ϕ, across the compressor. These are functions of frequency. The stationary value of the instantaneous pressure-ratio relationship provides the maximum excursion that then yields an expression for the planar-wave sensitivity of the compressor in terms solely of the phase change. Approximately, for small amplitude distortion, the sensitivity, S, is given as

$$S \approx \text{Sin } \Phi \qquad \text{(Eq. 3)}$$

The sensitivity, represented by the maximum instantaneous operating point pressure ratio change per unit planar-wave amplitude, is equivalent to the loss of stability pressure ratio, ΔPRS, per unit amplitude, consistent with the ARP1420 definition of sensitivity. At low frequencies, approaching zero, the compressor phase shift, f, tends to zero and the sensitivity tends to zero. For a typical compressor with a time constant, τ, of 3 ms:

f = 10 Hz ϕ = 10.7° S = 0.19
f = 20 Hz ϕ = 20.7° S = 0.35

The results of Equation 3 when plotted give the results shown in Figure 16. It is important to note that at zero frequency, the sensitivity is zero, that is, the discharge pressure of the compressor stays in phase with the inlet pressure to the compressor resulting in no loss of stability pressure ratio.

The planar wave amplitude at the stability limit as a function of frequency for an assumed compressor having a 10% available ΔPRS installed in a system characterized by a 3 ms time constant (Appendix B) is shown in Figure 17. As frequency increases and compressor planar-wave sensitivity increases (Figure 16), the acceptable planar wave amplitude is reduced. This reflects the increased phase shift across the compressor.

The above construction assumes that the clean-flow stability limit line may be used for the assessment of planar wave tolerance and further, that the compressor stages operate in a quasi-steady manner so that fixed-throttle stage matching at instability onset is preserved. This latter assumption is valid only at low frequencies and disturbance amplitudes. At higher frequencies, the stages become mismatched dynamically as a consequence of compressor blade-row and inter-row volume lags. In these circumstances, the clean-flow compressor stability limit line may be exceeded transiently and hence, may not be used to assess instability onset.

More sophisticated models applied to axial flow turbomachines solve simultaneously the one-dimensional unsteady-flow conservation equations, as stated earlier. Lumped-volume stage-by-stage predictions of planar-wave amplitude, required to stall a compression component for various frequencies in the range 0 to 70 Hz, are shown in Figure 18. Each compression component has different system dynamic characteristics. Note that all the compression components exhibit the same general trend and that agreement with the simple model discussed earlier is good.

The results extend the range of the simple model. It should be noted that the tendency for the surge tolerance curves of Figure 18 to rise at higher frequencies for the longer 11-stage and 15-stage compressors reflects stage mismatching across the units, and that the frequency range for the long dual-spool arrangement is insufficient to reach a minimum.

The evaluation of the response of a compression system to an arbitrary periodic wave by means of a generic sensitivity or ΔPRS derived by harmonic summation is clearly impossible as each wave will have a unique frequency and phase content. In contrast, a defined, specific wave is amenable to treatment. High-order computer models of the fan, compressor or spool-coupled compression system are available to estimate the destabilizing effect of the defined wave. The models utilize overall compressor characteristics, stage-by-stage, or blade-row simulations and one-dimensional, unsteady gas dynamics (6.3). The results of an estimate for the effects of the periodic wave example illustrated in Figure 19 are shown in Figures 20 and 21. The model employed a lumped-volume representation of the one-dimensional flow-conservation equations in a spool-coupled compression system comprised of a fan and high-pressure compressor. Time variations in the stability margins of the fan (Figure 20) and the HPC (Figure 21), expressed in terms of available ΔPRS at a flow, are shown. In this example, the available ΔPRS dropped from the initial, undistorted values of 17% and 21% for the fan and HPC to 8% and 16%, respectively. That is, peak ΔPRS losses for the fan and HPC were about 10% and 5% for the planar wave having a maximum peak-to-peak magnitude of 16%.

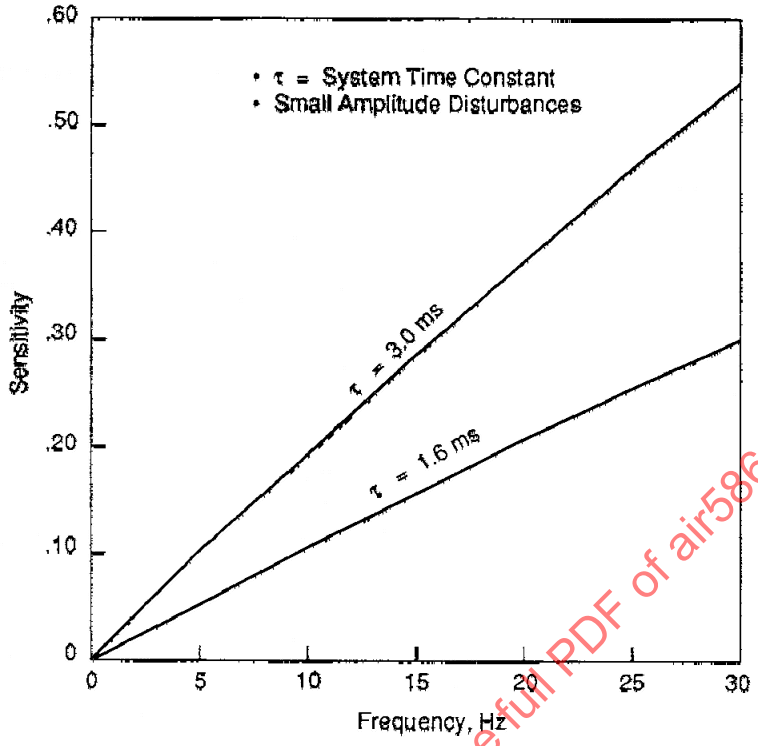

FIGURE 16 - PLANAR WAVE SENSITIVITY, SIMPLE ILLUSTRATIVE ANALYSIS

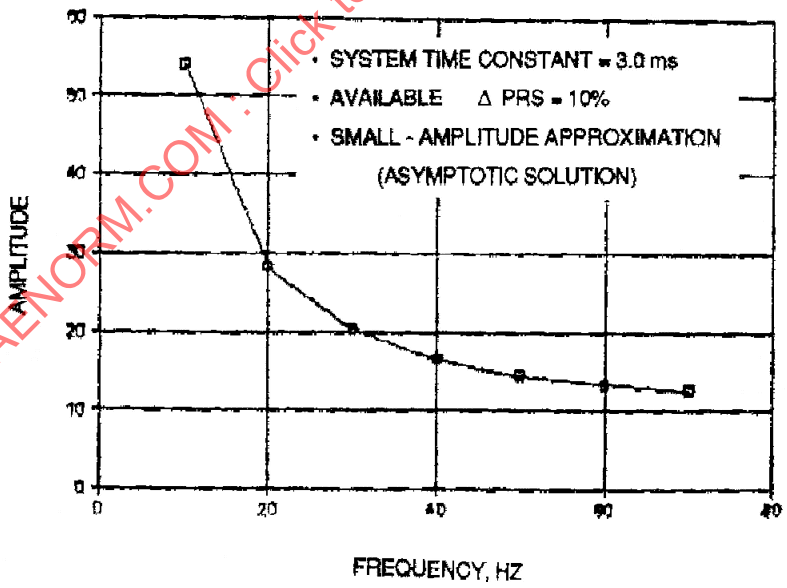

FIGURE 17 - PLANAR-WAVE SENSITIVITY, AMPLITUDE TO STALL

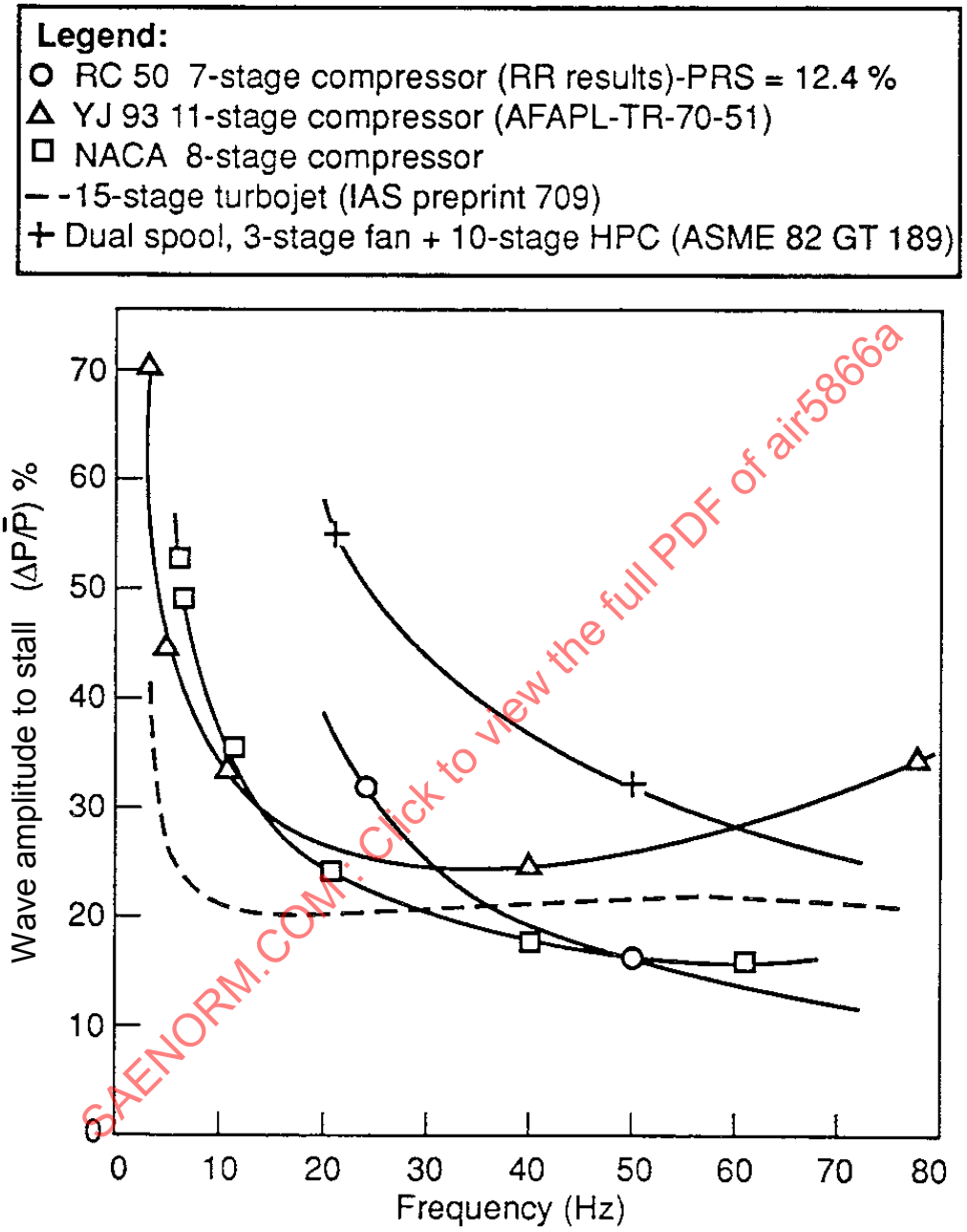

FIGURE 18 - INLET PLANAR PRESSURE WAVE - PREDICTED AMPLITUDE TO CAUSE STALL, SINE WAVES

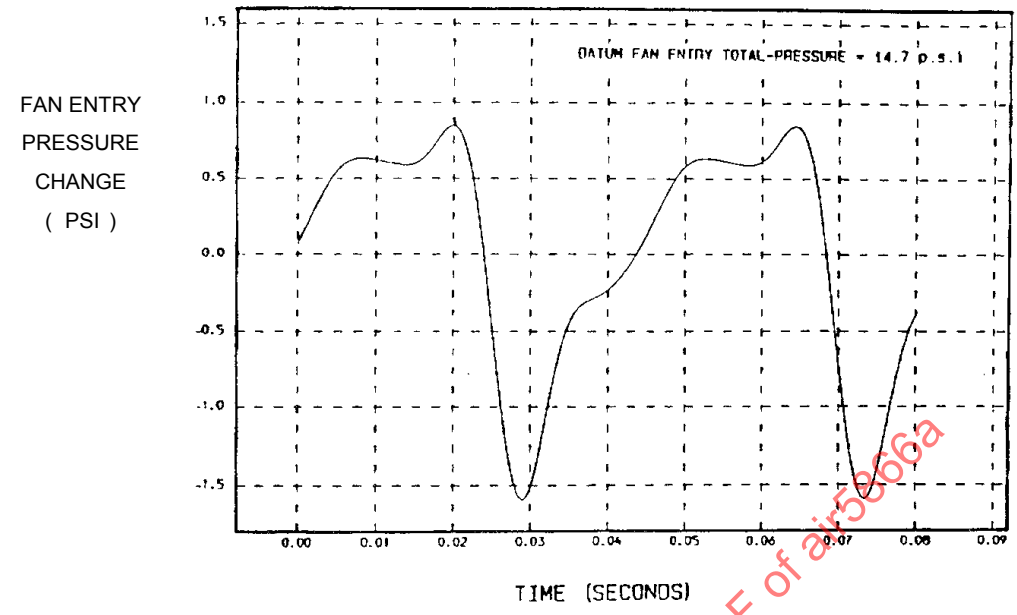

FIGURE 19 - PERIODIC PLANAR WAVES, INLET TOTAL-PRESSURE DISTORTION (EXAMPLE)

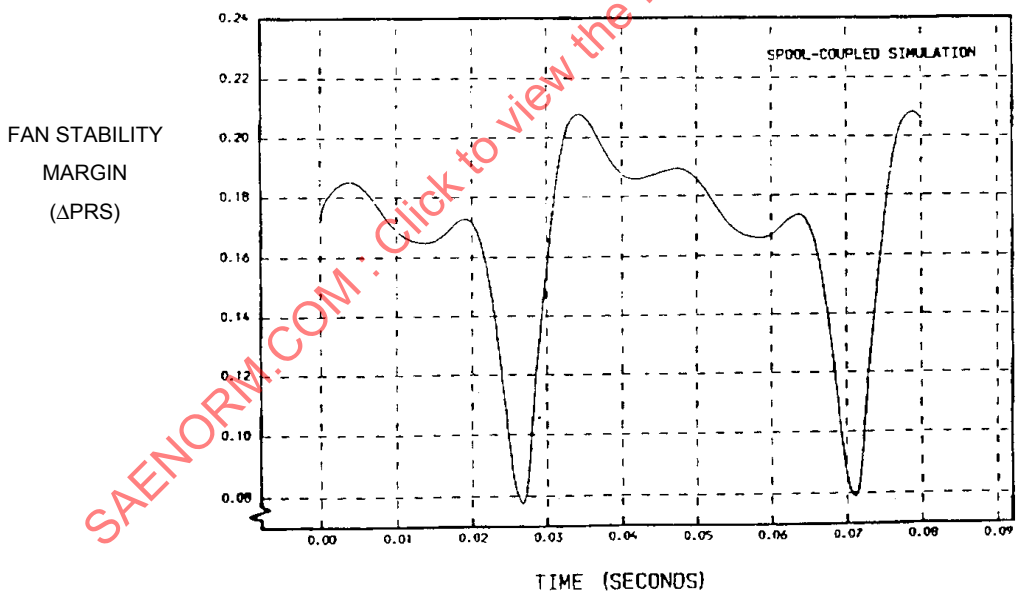

FIGURE 20 - PERIODIC PLANAR WAVES, FAN STABILITY MARGIN VARIATION (EXAMPLE)

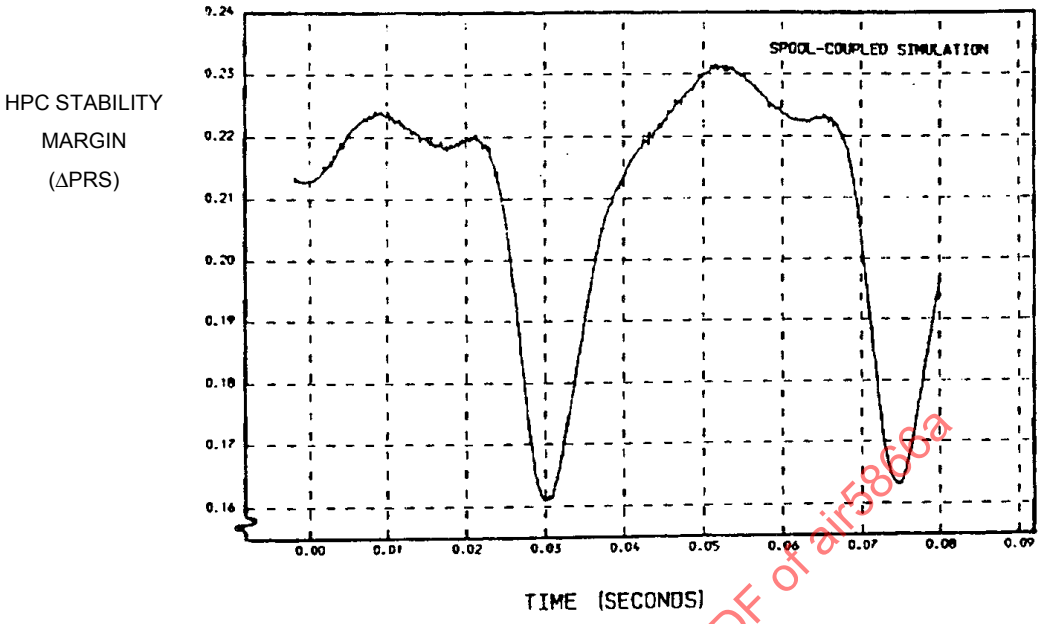

FIGURE 21 - PERIODIC PLANAR WAVES, HIGH PRESSURE COMPRESSOR STABILITY MARGIN VARIATION (EXAMPLE)

6.3 Planar Wave Methodology Approaches

Because inlet data obtained from the standard forty-probe AIP array are used, additional data gathering and analysis efforts have been minimized. Further, the definition of Equation 1 assures that spatially random events (from one side of the inlet to the other) will be averaged out and components of the time-varying total pressure will be those that act in unison over the whole engine face. Having defined what is meant by a planar wave, the task now becomes that of defining the response of the compression system or turbofan engine to a planar wave, that is, what is the loss of stability pressure ratio attributable to the presence of a planar wave at the engine face.

Currently, there are two methods (though not unrelated) for assessing the loss of stability pressure ratio due to planar waves. One method uses the planar waveform (defined by Equation 1) as input to a computer simulation of the compression system or engine and the second uses a sensitivity analysis. Each has its utility as discussed below.

6.3.1 Computer Simulation Prediction

If an appropriate computer simulation exists for the compression component or engine of interest, the average time-varying total-pressure waveform (as defined by Equation 1) can be used as input to the computer simulation. By throttling each compression component to aerodynamic instability, the loss of stability pressure ratio at constant corrected flow measured from the average compression-component operating point to the clean stability limit line can be determined for the given corrected speed. This assumes that the computer model has frequency response capability in excess of the highest frequency content contained in the planar wave of interest.

6.3.2 Sensitivity Analysis

If one were interested in screening a large amount of inlet data to assess the impact of planar waves on inlet-engine compatibility, the sensitivity approach as reported in Reference 2.2.7 would be appropriate. Further, this approach provides a method for generalizing planar wave test data. This sensitivity approach is similar to the distortion sensitivity approach used to analyze the circumferential and radial components of spatial total-pressure distortion. The sensitivity of a compression component to the loss of stability pressure ratio due to the presence of time-varying planar total-pressure waves as a function of frequency has been determined both experimentally and by the use of digital computer simulations. In both of these cases, the sensitivity to planar waves was reported as a loss in stability pressure ratio per unit planar wave amplitude (one-half of the peak-to-peak value) at each given frequency as follows:

$$K_P(f) = \Delta PRS / AMP \quad \text{(Eq. 4)}$$

An example of the sensitivity of a large two-stage fan to inlet total-pressure waves is presented in Figure 22 as taken from Reference 2.2.8.

The results of several unpublished computer simulations and the modeling discussed in 4.2.3 show that the sensitivity function of Figure 22 goes to zero at zero frequency. Therefore, based on the results of these studies, the results of Figure 22 have been extended using the computer simulation results in the low-frequency range, and fairing the computer and experimental results together in the 30 to 40 Hz range. The sensitivity function obtained in this manner is shown in Figure 23.

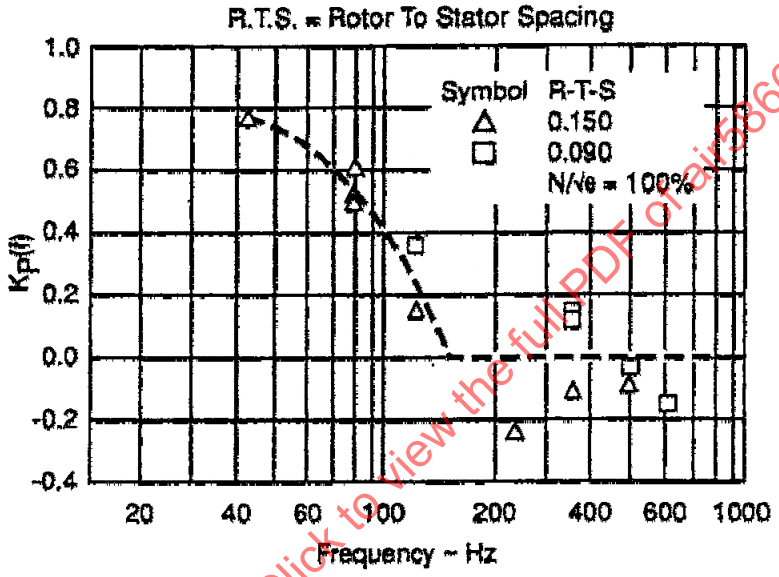

FIGURE 22 - DYNAMIC DISTORTION SENSITIVITY VERSUS FREQUENCY - N/√θ = 100%

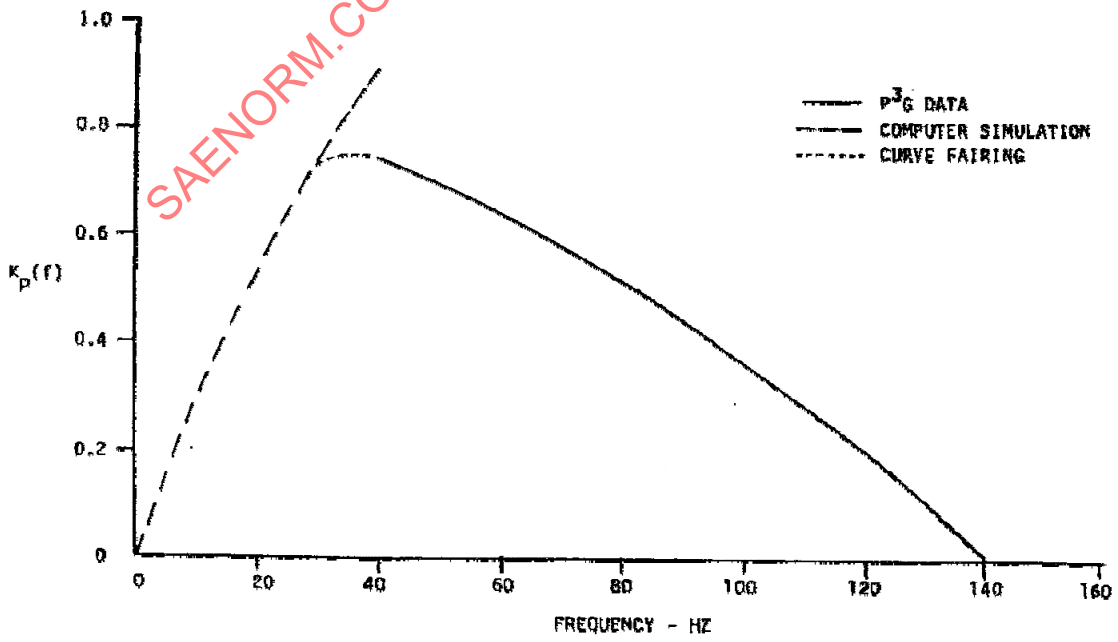

FIGURE 23 - FAN-COMPONENT PLANAR-WAVE SENSITIVITY

The root-mean-square response of a compression component to inlet planar waves can be formulated using the power spectral density of the inlet planar wave (input) and a compression component sensitivity to planar waves that is a function of frequency (gain factor) as follows:

$$\Delta PRS_{RMS} = \left[\int_0^{\infty} \left[\phi(f) * K_P^2\ (f)\ df\right]\right]^{1/2} \quad \text{(Eq. 5)}$$

where $K_p(f)$ is a sensitivity and ΔPRS_{RMS} is the root-mean-square loss of compression component stability pressure ratio due to inlet total-pressure waves. (For additional details, the reader should consult Reference 2.2.7). Hence, because this is a generalized formulation, it is applicable to inlet planar total-pressure waves with arbitrary frequency content, that is, random, periodic (pure or harmonic), or any combination thereof. For specific types of waveforms, Equation 5 can be shown to reduce to simpler expressions that aid interpretation.

The root-mean-square loss of stability pressure ratio as expressed by Equation 5 can be obtained in a straightforward manner. The power spectral density function $\Phi(f)$ is obtained from the engine-face spatially averaged total-pressure waveform given by Equation 1. Equation 4 gives the sensitivity of the compression component to planar waves. The sensitivity of Equation 4 appears as a squared term in Equation 5 to maintain consistency of units.

All that now remains is to determine the relationship of the peak loss of stability pressure ratio to the root-mean-square loss of stability pressure ratio.

For engine-face planar waves that are pure sinusoids with frequency f, it can be shown that

$$\Delta PRS_{rms} = K_P(f) \bullet \hat{P}(t)_{rms} \quad \text{(Eq. 6)}$$

and the peak loss of stability pressure ratio is given by

$$\Delta PRS_{peak} = \frac{K_P(f) \bullet \hat{P}(t)_{rms}}{0.707} \quad \text{(Eq. 7)}$$

For engine-face periodic waves with harmonic content, the relationship between the peak loss of stability pressure ratio and the root-mean-square loss of stability pressure ratio is more complex and can be determined from Fourier series analysis for the specific engine-face planar wave form if the situation warrants.

For engine-face planar waves that are random in content, the situation is complicated by the fact that the sensitivity is a highly non-linear function. Thus the loss of stability pressure ratio as a function of time is not random and one cannot make the assumption that Gaussian statistics apply. The immediate implication of these facts is that the one, two, and three standard deviation (rms) levels do not have their usual 84.1, 97.7, and 99.9% occurrence representations, respectively. However, it is still possible to bound the peak level of loss of stability pressure ratio as follows.

$$\Delta PRS_{peak} = C_R \bullet \Delta PRS_{rms} \quad \text{(Eq. 8)}$$

C_R is defined as the “crest factor” for random waves. Studies will have to be accomplished to determine the magnitude of C_R that encompasses the peak loss of stability pressure ratio for approximately 99% of the time. It is thought that since the sensitivity function attenuates the high frequency components, the factor C_R will have a value considerably less than 3.0. A value of 2.0 (based on judgment) is recommended until further studies can be conducted to provide a more refined value. Validation and use of this methodology are presented in Appendix C.

6.4 Combined Spatial Total-Pressure Distortion and Planar Waves

Any methodology for handling planar waves must also address the manner in which any concomitant time-varying spatial distortion is to be assessed. The methodology should assure that both stability limit line and operating line effects would be taken into account in any stability assessment.

Because of the complexities noted above, the planar-wave analysis problem was divided into a number of analytical sub-problems that would permit different simplifying assumptions to be employed depending on the frequency range of interest and the level of spatial total-pressure distortion present. The summary shown in Figure 24 for the purposes of illustration represents choices that are by no means unique. Other investigators may choose to subdivide the problem in a different manner. Examination of the chart will reveal that the intent is to take advantage of regions where linear superposition should be valid.

Case A represents the situation where planar waves are not present (or are present to an insignificant extent) and the ARP1420 methodology for spatial total-pressure distortion is all that is required. Case B represents the situation where there is no significant spatial distortion present and the planar wave has low frequency content. Case C represents the situation where the planar-wave frequencies including harmonics are low and spatial total-pressure distortion is present. Case D applies to those situations where planar-wave frequency content exists over the sensitive range of the compression component, but no significant total pressure distortion is present. Case E addresses the situation where both planar waves and spatial distortion are present and the regions where linear superposition of both the planar-wave stability-pressure-ratio loss and the spatially total-pressure distortion loss can be assumed. For completeness, Case F addresses those situations where nonlinearities can be expected to significantly influence the results. Under these conditions, it is highly probable that linear superposition cannot be used to give appropriate estimates of loss of stability margin.

With this background, it is appropriate to briefly review and bring together those elements of spatial total-pressure distortion (ARP1420) that will be used to provide a full accounting for combined spatial total-pressure distortion and planar waves.

6.4.1 Spatial Distortion

Guidelines for assessment of the effects of spatial time-variant total-pressure distortion on gas-turbine engine stability and performance are provided in ARP1420 and the companion report AIR1419. Three circumferential distortion elements - intensity, extent and multiple-per-revolution, and one radial distortion element are identified for use as inlet distortion descriptors using AIP measurements for each measurement ring.

$$\text{Circumferential Intensity, } (\Delta PC / P)_i = \frac{(PAV)_i - (PAVLOW)_i}{(PAV)_i} \quad \text{(Eq. 9)}$$

$$\text{Circumferential Extent, } (\theta^-) = \theta_{2i} - \theta_{1i} \quad \text{(Eq. 10)}$$

$$\text{Radial Intensity, } (\Delta PR / P)_i = \frac{(PFAV) - (PAV)_i}{(PFAV)} \quad \text{(Eq. 11)}$$

The Circumferential Intensity and Extent Elements are illustrated in Figure 25 for a one-per-revolution total-pressure distortion pattern.

The Radial Intensity is illustrated in Figure 26 for the tip-radial distortion pattern.

The Circumferential Multiple-Per-Revolution element MPR is formulated on an instrumentation ring basis and treats patterns having several low total-pressure regions either as an equivalent one-per-revolution pattern or as a factor on the maximum low-pressure region, depending on the structure of the distortion (Reference 2.2.1).

Case	Frequency of planar-wave content	Spatial distortion levels present $\frac{\Delta PC}{P}$, $\frac{\Delta PR}{P}$	Analytical techniques		Comments
			Stability limit line effects	Operating line effects	
A	None	Any levels	ARP 1420 methodology for distortion	Current methods for distortion if any effect	Current practice
B	<20 Hz*	None	Transient deck ** to determine planar-wave sensitivity	Transient deck ** to determine maximum operating line migration	• Transient deck to predict sensitivity must have stall prediction capability • Operating line migration can be determined by using $\eta(t)$ as input
C	<20 Hz*	Any levels	• Transient deck ** to determine planar-wave sensitivity plus • ARP 1420 methodology for distortion	• Transient deck ** to determine maxium operating line migration plus • Current methods for distortion if any effect	Same as above
D	20 Hz* to rotational speed equivalent	None	• Transient deck ** with stage-by-stage compression component representation or test to determine sensitivity	• Transient deck ** with stage-by-stage compression component representation to determine unsteady operating line migration	Same as above
E	20 Hz* to rotational speed equivalent	$\frac{\Delta PC}{P} \le 0.09$ and/or $\frac{\Delta PR}{P} \le 0.06$	• Transient deck ** with stage-by-stage compression component representation or test to determine sensitivity plus • ARP 1420 methodology for distortion	• Transient deck ** with stage-by-stage compression component representation to determine unsteady operating line migration plus • Current method for distortion if any effect	Same as above
F	20 Hz * to rotational speed equivalent	$\frac{\Delta PC}{P} > 0.09$ and/or $\frac{\Delta PR}{P} > 0.06$	Due to nonlinear effects, linear superposition becomes more suspect		Consensus technology does not exist

Legend:
* Nominal value
** Transient deck configuration with respect to performance and unsteady aerodynamic consistent with the problem being addressed.

FIGURE 24 - CATEGORIZATION OF ANALYTICAL TECHNIQUES

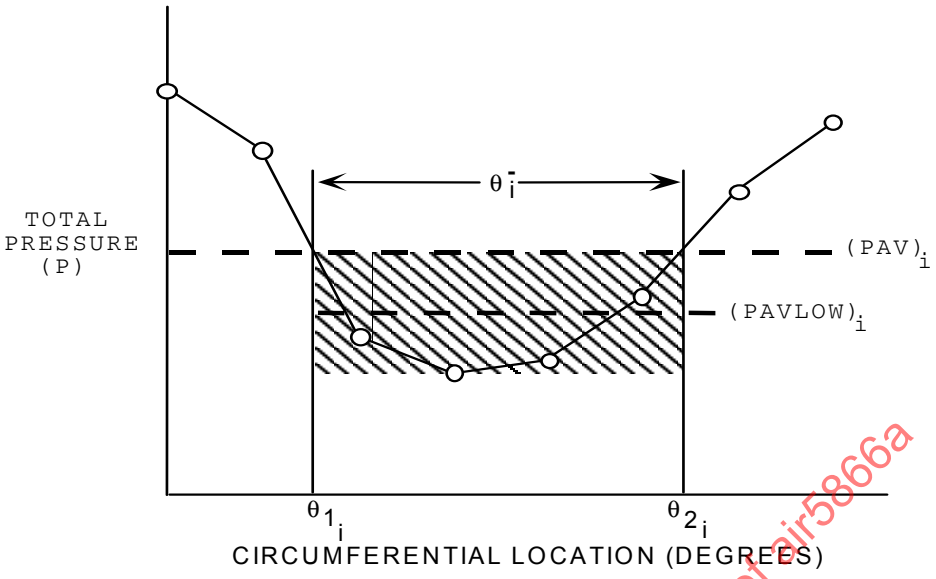

FIGURE 25 - RING CIRCUMFERENTIAL DISTORTION (ONE-PER-REV-PATTERN)

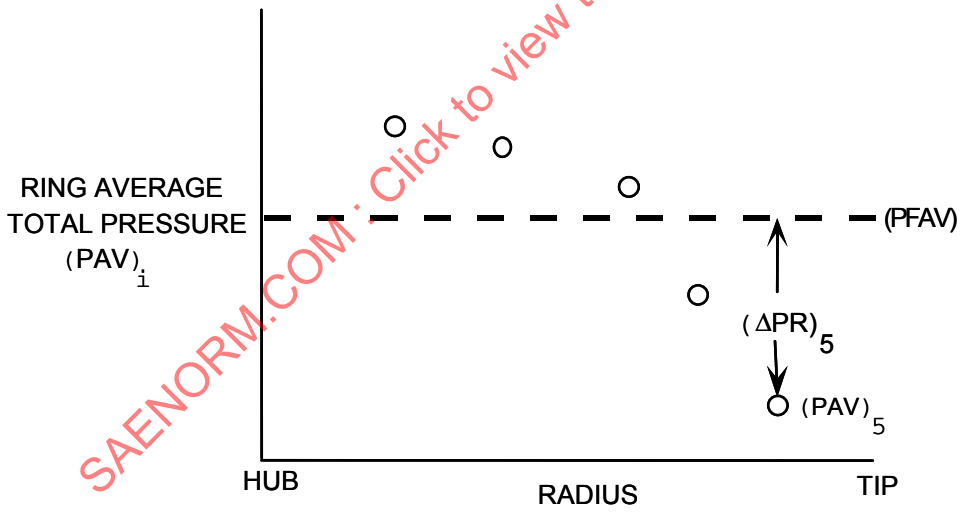

FIGURE 26 - RADIAL DISTORTION PATTERN

The spatial distortion descriptor elements can be related to the loss of compressor stability pressure ratio by the general relationship

$$\Delta PRS = \sum_{i=1}^{N} \left[KC_i (\Delta PC / P)_i - KR_i (\Delta PR / P)_i + C_i \right] \times 100 \quad \text{(Eq. 12)}$$

where:

ΔPRS = loss of stability pressure ratio due to the spatial distortion, expressed as a percent of the undistorted stability pressure ratio

N = number of AIP instrumentation rings

KC = generalized circumferential distortion sensitivity

KR = generalized radial distortion sensitivity

C = an offset term

The sensitivities and offset coefficients vary with distortion (extent, multiple-per-rev, etc.), compression system design, and operating conditions. Downstream compression components are treated according to Equation 10 using distortion transfer characteristics across upstream compressor components.

6.4.2 Stability Margin

The ARP1420 definition of stability margin (Figure 27) is

$$\Delta SM = ((PR1 - PRO) / PRO) \times 100 \quad \text{(Eq. 13)}$$

The stability margin is defined at the operating airflow and normalized by the operating pressure ratio.

The loss of stability pressure ratio (ΔPRS) due to the spatial total-pressure distortion (Figure 27) is

$$\Delta PRS = ((PR1 - PRDS) / PR1) \times 100 \quad \text{(Eq. 14)}$$

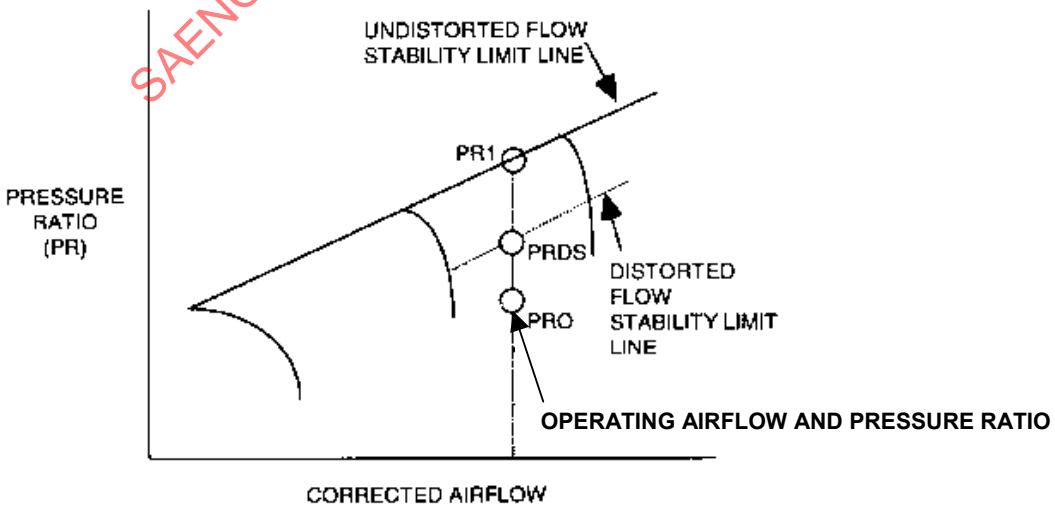

FIGURE 27 - STABILITY MARGIN DEFINITION

In the case that planar wave distortion arises, then PRO and corrected airflow vary with time. The impact on stability margin accounting is discussed in 6.4.3. Where compression component geometry is set by gas-path sensors which respond to planar-wave disturbances, variations in the compression component map will occur and will affect the stability margin accounting.

6.4.3 Stability Margin Accounting

A consensus method that accounts for the effects of combined planar waves and spatial distortions on engine stability has yet to be established. As shown earlier (Figure 24), various categories of problem and analysis techniques arise, each requiring individual treatment. Two general approaches to the problem of quantifying the loss of stability can be made. These two approaches arise as a result of the choices available for defining the face-average total pressure, PFAV. The choices available for PFAV are (1) the time-variant face-average pressure $PFAV_{TV}$ or (2) the time-averaged (steady-state) value of the face-average pressure $PFAV_{ss}$. Care must be exercised in defining $PFAV_{SS}$. A rigorous definition of $PFAV_{SS}$ requires that the time-dependent values be integrated over an infinite time span. For practical cases, such an interval is not possible and an approximation must be used. For the case of planar waves, the integration interval should be selected to be consistent with engine system responses including controls and the frequency of the planar wave. The interval selected will likely be empirical and dependent on the particular characteristics of the engine being evaluated.

In ARP1420, spatial time-variant distortion was described. This is a sufficient description of the flow quality at the AIP when the fluctuations in PFAV or planar wave amplitudes due to intake turbulence are sufficiently small that the planar wave content is negligible. In such cases, the values of the time-variant ring-average pressures $(PAV)_i$ in some sense cancel, as might occur in the turbulent flow at the AIP, so that their sum does not vary significantly. This cancellation becomes increasingly unlikely as cross-correlations between probes, reflecting a growth in turbulence eddy sizes, increase. A larger planar wave component would then arise.

If the selected descriptor system is based on the time-variant face-average pressure $PFAV_{TV}$, then the destabilizing effect of the spatial distortion on the compression system, ΔPRS, can be accounted for using the conventional sensitivity procedures of ARP1420 and AIR1419. An additional descriptor with a separate compression-system ΔPRS sensitivity would need to be developed to account for the destabilizing effect of the planar wave. The total ΔPRS due to the combined spatial distortion and planar wave would be accounted for by some form of superposition and the system can be termed a “two-parameter system”. The superposition procedure would need to take into consideration the time-phasing between peaks and troughs in the spatial distortion and the PFAV fluctuations.

If the selected descriptor system is based on steady-state face-average pressure $PFAV_{ss}$, then the destabilizing effect of the combined spatial distortion and planar wave is accounted for in one descriptor and the methodology can be termed a “one-parameter system”. Compression-system ΔPRS can then be accounted for using a composite sensitivity that includes planar-wave and spatial distortion sensitivities. Separate ΔPRS accounting for the planar wave is not necessary. In this case, the combinational algebra lies within the engine distortion-response algorithm.

In the general case of combined spatial distortion and planar wave, both forms of destabilizing disturbances can cause losses of stability pressure ratio (ΔPRS) and shifts in mean operating line point, PRO, of Figure 27.

At low frequencies, the loss of compressor stability pressure ratio due to planar waves may be accounted for entirely by examining the movement of the transient operating point. However, as the frequency increases, the transient operating point can exceed the clean-inlet-flow steady-state stability limit line for increasing amounts of time without incurring an aerodynamic instability. At sufficiently high planar-wave frequencies, the mean operating point can lie on or almost on the clean-inlet-flow stability-limit line without incurring any loss of stability pressure ratio although the transient operating point may spend a major portion of a planar wave cycle above the clean inlet flow stability-limit line. Under these circumstances, the loss of stability pressure ratio is a function of frequency and must be accounted for accordingly. In the cases that are encountered most often, the frequencies are low, being those associated with buzz or subsonic low-flow instability.

6.4.3.1 Two-Parameter Approach

The total loss of compression-component stability margin can be accounted by assessing the loss of stability pressure ratio due to the spatial distortion and treating the effect of the planar wave as a rise in operating-point pressure ratio, as illustrated in Figure 28. PRDS represents the stability pressure ratio in the spatially-distorted flow and PRDO represents the raised operating pressure ratio due to the planar wave, both being defined at constant inlet corrected airflow, consistent with ARP1420 methodology. Both pressure ratios represent the maximum-loss values in the time-variant process. For the planar-wave excursion, the actual trajectory of the transient operating point may involve changes in corrected airflow, as illustrated schematically in Figure 29 for a sinusoidal planar wave. PRDO, defined at constant corrected flow, WC, represents the peak of the time-variant pressure-ratio loop.

The loss of stability margin is approximately proportional to the sum of the changes in stability-limit-line and operating-line pressure ratios due to the spatial distortion and the planar wave, respectively.

The loss of stability due to the spatial distortion is fully described in the methodology of ARP1420 and AIR1419. That due to the planar wave is described in 6.2 and 6.3 of the present report. For some purposes, it is convenient to convert the planar-wave ΔPRO to an equivalent loss of stability pressure ratio. This is accomplished readily by means of the relation:

$$\Delta PRS = \frac{\Delta PRO}{1 + SM} \quad \text{(Eq. 15)}$$

where, ΔPRS is defined by:

$$\Delta PRS = \left(\frac{PRDO - PRO}{PR1} \right) \times 100 \quad \text{(Eq. 16)}$$

and ΔPRO is given by:

$$\Delta PRO = \left(\frac{PRDO - PRO}{PRO} \right) \times 100 \quad \text{(Eq. 17)}$$

Hence, the conversion from ΔPRO to ΔPRS involves a change only in the undistorted flow reference pressure ratio from PRO to PR1.

The total loss of compression-system stability can then be expressed consistently as:

$$\Delta PRS_{TOTAL} = \Delta PRS_{PLANAR} + \Delta PRS_{SPATIAL} \quad \text{(Eq. 18)}$$

The equations above describe the fundamental approach to the accounting of the destabilizing effect of combined planar waves and spatial distortion. The description is based on synthesizing the total loss of stability margin from the individual destabilizing factors in the overall distortion.

It is important to recognize that what matters is the total loss of engine stability and that, in some instances, in particular those where spatial distortion and planar-wave amplitudes and waveforms are large and complex, e.g., case F of Figure 24, it may be difficult to separate the individual effects, as described, from the time-variant inlet distortion ahead of the installed engine. Here, linear superposition, as illustrated by the previous equation, cannot be used.

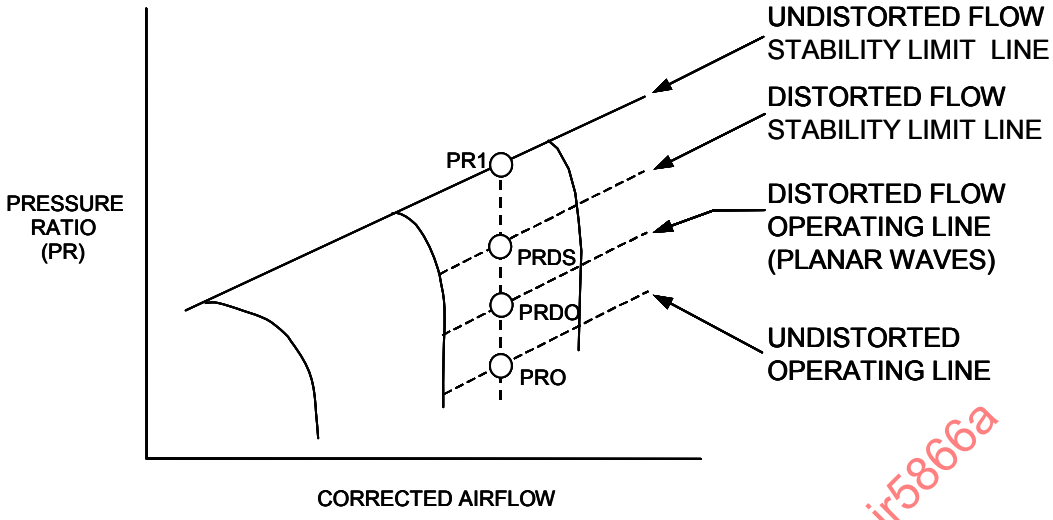

FIGURE 28 - COMBINED PLANAR WAVE AND SPATIAL DISTORTION

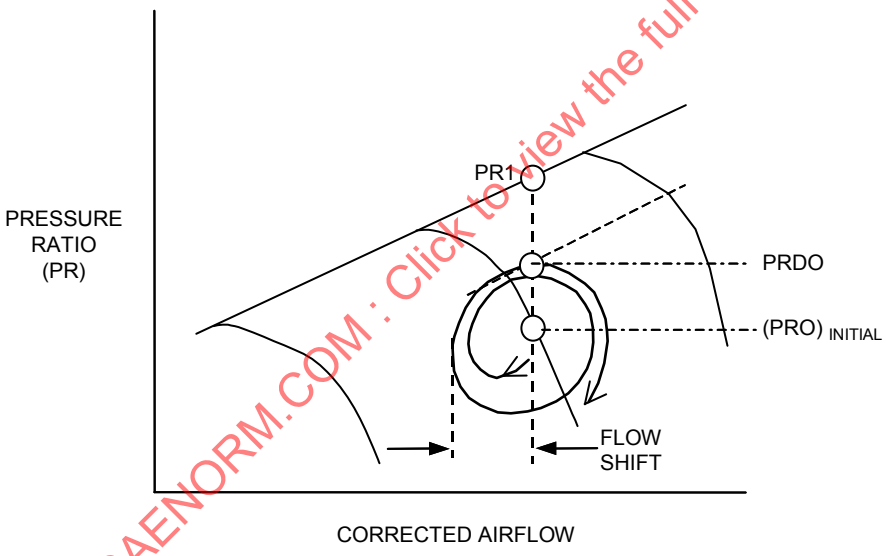

FIGURE 29 - COMPRESSOR OPERATING - POINT EXCURSION-PLANAR WAVE SINUSOID

The ΔPRS due to spatial distortion can be related to the spatial distortion at the AIP using the ARP1420 distortion elements. The general relationship for ΔPRS is given by Equation 12 (Paragraph 6.4.1). The ΔPRS due to the planar wave may be related to an appropriate wave amplitude by a relevant distortion sensitivity: Equations 4 to 8 (6.3.2). As stated earlier, this approach necessitates accounting for the combined distortion using separate descriptors for spatial distortion and for planar waves, their respective sensitivities with the spatial distortion descriptor being consistent with ARP1420 methodology.

The planar wave descriptor or intensity element will be defined from the time-variant, face-average total pressure $PFAV_{TV}$ and the steady-state average total pressure $PFAV_{SS}$ in a manner consistent with the planar-wave methodology of 6.3. For a simple sinusoidal disturbance, this element (e.g., AMP, Equation 4, 6.3.2) may be defined as the “amplitude” (one half of peak-to-peak value) of the disturbance as:

$$AMP = (PFAV_{SS} - PFAV_{TV}) / (PFAV_{SS}) \quad \text{(Eq. 19)}$$

The benefits of the two-parameter approach are threefold: (1) The definitions and stability accounting remain consistent with ARP1420 and AIR1419 documentation, (2) new data remain consistent with past data bases, and (3) the impact of time-variant spatial distortion and planar waves can be separately identified. The latter is important since the inlet design factors that can influence inlet/engine incompatibility due to combined spatial and planar distortion, in each case can differ significantly.

Reference 2.2.7 is an example in which planar waves were analyzed giving a more realistic insight into the impact of planar waves.

6.4.3.2 One-Parameter Approach

In this approach, the descriptor system is defined such that all spatial and time-variant perturbations in total pressure from steady, uniform-flow conditions at the AIP are accounted relative to the steady-state, face-average total pressure, $(PFAV)_{SS}$.

Separate accounting of the planar-wave and spatial disturbances is dispensed with, and in this sense, the system can be said to provide a “one-parameter” approach to the unsteady-flow problem. As the distortion descriptor (or possibly fan and core-engine descriptors in the case of the two-stream turbofan engine) is no longer concerned exclusively with spatial distortion, the distortion elements defined in ARP1420 are not applicable directly and extended definitions are needed. This need is a consequence of the avoidance of a separate and additional element, or elements, to describe the planar wave. The approach constitutes a global description of the combined planar wave/spatial distortion problem.

Composite Descriptor

The general nature of the method of describing the distortion at the AIP is best explained by means of an example. Inlet total-pressure-distortion data presented in Figure 30 show a large planar-wave disturbance co-existing with time-variant spatial distortion. The time traces derive from a supersonic wind-tunnel test of a sub-scale model of a combat aircraft at Mach 2. The upper curve shows the variation of the face-average total pressure, $(PFAV)_{TV}$, with time plotted relative to the steady-state or time-average total pressure, $(PFAV)_{SS}$. Significant troughs in the curve occur and these act to destabilize the engine. The lower curves show the variations with time of a spatial-distortion descriptor, based on $(PFAV)_{TV}$, and of a composite descriptor based on $(PFAV)_{SS}$. The former time trace exhibits the characteristic randomness that is typical of turbulence-induced spatial distortion, while the latter, composite time-trace captures the planar-wave component of the overall distortion.

A noteworthy feature of the data record is that the peak of the composite descriptor coincides with the minimum of the trough of the planar-wave disturbance. This occurred because, in this case, the planar-wave oscillation dominated the total disturbance as can be seen from the magnitudes of the individual terms. In cases where the levels of the planar-wave and spatial distortion disturbances are comparable, the peak of the composite descriptor corresponds neither to a peak of the spatial-distortion descriptor nor to a minimum of the planar-wave so that significant phase differences occur between the distortion components (it is this difference that has to be accounted for in the two-parameter approach to the combined distortion problem).

The composite descriptor, DP_{COM} can be expressed in terms of the steady face-average pressure and an average low total pressure, defined to encompass the total-pressure defect region of interest, as:

$$DP_{COM} = (PFAV_{SS} - PAVLOW_{TV}) / (PFAV)_{SS} \quad \text{(Eq. 20)}$$

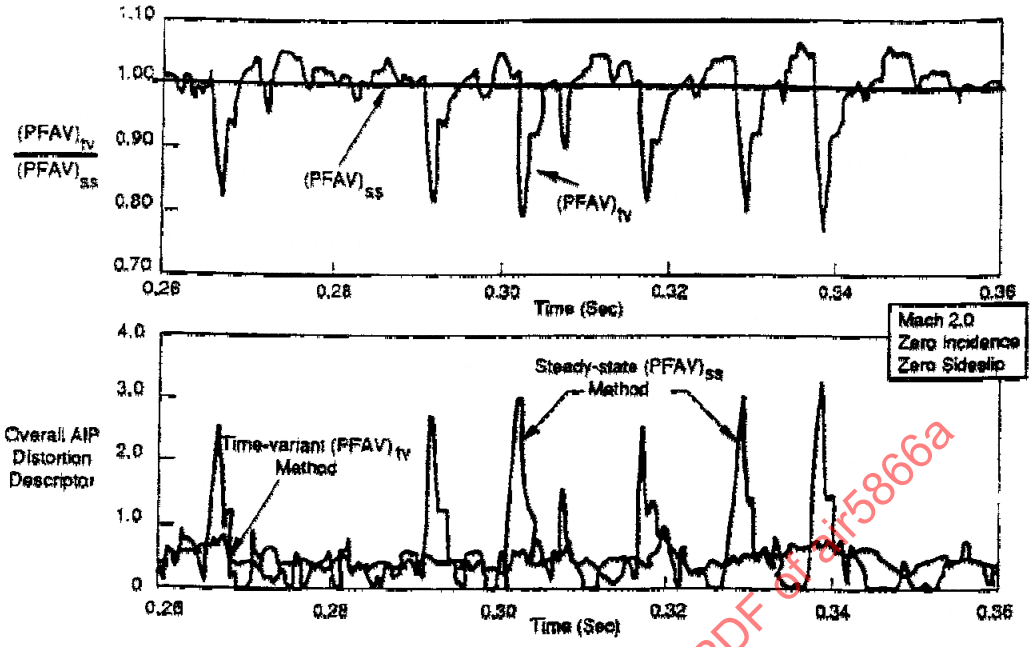

FIGURE 30 - AIR-INTAKE TIME-VARIANT SPATIAL DISTORTION WITH EMBEDDED PLANAR WAVE

Here, the average low total pressure, $PAVLOW_{TV}$, is defined as the time-variant minimum pressure, in the usual way, for an appropriate region of the AIP.

An example, illustrating a descriptor defined over the whole of the AIP for a one-per-rev spatial distortion pattern is shown in Figure 31. The average minimum pressure is defined to lie within a circumferential sector of extent $\bar{\theta}_{AV}$.

The corresponding time-variant spatial-distortion descriptor, DP_{SP}, is in this case, given by:

$$D_{SP} = (PFAV_{TV} - PAVLOW_{TV}) / (PFAV)_{TV} \quad \text{(Eq. 21)}$$

where the steady face-average pressure in the composite descriptor has been replaced by the time-variant, face-average pressure.

By defining the planar-wave intensity element, $(\Delta P/P)_{PW}$, as:

$$(\Delta P / P)_{PW} = (PFAV_{SS} - PFAV_{TV}) / (PFAV)_{SS} \quad \text{(Eq. 22)}$$

the relationship between the composite and the time-variant spatial-distortion descriptors can easily be shown to be given by:

$$\underset{\text{COMPOSITE}}{DP_{COM}} = \underset{\text{SPATIAL}}{[1 - (1 - DP_{SP})]} \times \underset{\text{PLANAR}}{[1 - (\Delta P / P)_{PW}]} \quad \text{(Eq. 23)}$$

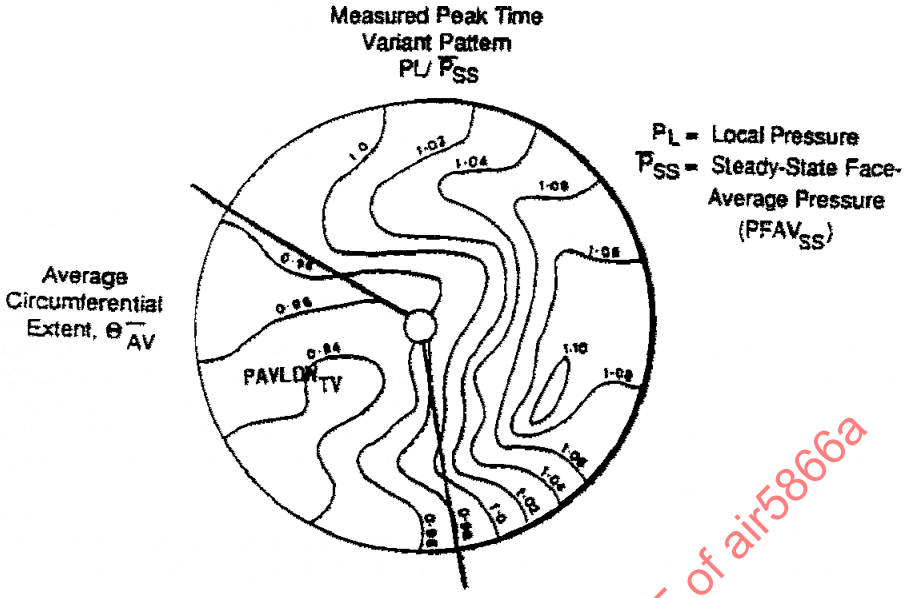

FIGURE 31 - COMPOSITE DISTORTION DESCRIPTOR-OVERALL FACE

All the parameters apply “instantaneously” to each time-slice of the time-variant pressure record. By inspection of the above expression, it may be seen that for the case of zero spatial distortion, $DP_{SP} = 0$, we have:

$$DP_{COM} = (\Delta P/P)_{PW} \quad \text{(Eq. 24)}$$

For the case of zero planar-wave intensity, $(\Delta P/P)_{PW} = 0$, we have:

$$DP_{COM} = DP_{sp} \quad \text{(Eq. 25)}$$

As the intensity of the planar-wave disturbance increases, the level of the spatial distortion descriptor decreases for a fixed value of the composite descriptor. This is illustrated in Figure 32 where values of the composite descriptor are plotted in terms of the component intensities of the overall distortion as the dotted curves.

The solid lines of the figure represent an approximate relationship between the composite, spatial, and planar-wave terms obtained by neglecting second-order terms in the expansion of the right-hand-side of Equation 23. The composite descriptor is then the sum of the spatial-distortion and planar-wave descriptors and is thus a linear relationship. This relationship is consistent with the linearization of superposition processes and the limited size of terms allowable by the magnitude of compression-component available stability margins.

Alternatively, the linear relationship may be derived exactly by defining the spatial-distortion descriptor to be:

$$DP_{SP} = (PFAV_{TV} - PAVLOW_{TV}) / (PFAV)_{SS} \quad \text{(Eq. 26)}$$

by replacing the time-variant face-average pressure in the denominator of the spatial descriptor by the steady-state face-average pressure.

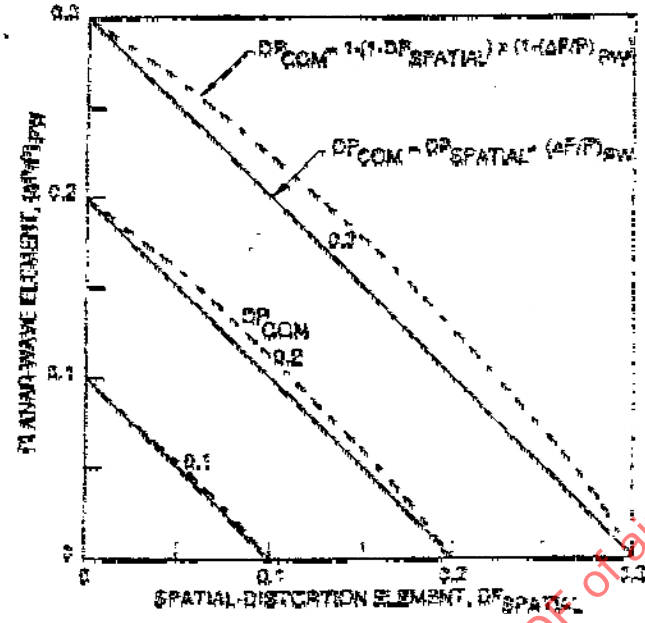

FIGURE 32 - COMPOSITE DESCRIPTOR, DP_{COM}

In the "one-parameter" system, the distortion tolerance of the engine at given operating conditions can be expressed in terms of the composite descriptor. The relationships illustrated in Figure 32 exemplify the equivalence between this description of the combined distortion and the separate planar-wave and spatial distortion description, and show the trade-off between planar-wave and spatial-distortion levels for a fixed, allowable composite-descriptor level.

It is important in constructing a descriptor system appropriate to a specific propulsion-system development to ensure consistency among the spatial-distortion and planar-wave elements of the combined distortion. In the two-parameter approach to the problem, the spatial-distortion elements are time-variant and consistent with the ARP1420 definitions. In the one-parameter approach, these may not apply and modified radial and circumferential intensity elements may be needed, depending on the accounting system adopted and on the sensitivity of the compression-system components to the combined distortion. Various options for combining the absolute, point pressure readings of the probes at the AIP will exist, as is suggested by the forms of the overall descriptor example provided earlier.

Compression-System Sensitivity

The composite descriptor used to describe the distortion limit of the engine provides a screening parameter for the engine inlet. In general, the stability response of the engine to the combined distortion will involve the whole engine, particularly at lower planar-wave frequencies up to 20 Hz or so, nominally, due to the effect of the wave on the operating lines of the components of the engine and the transient rematching of the components. This situation differs from that of the pure time-variant, spatial distortion case where the effect of the spatial distortion on the stability of the engine is almost entirely dictated by the response of the compression-system components.

Bearing in mind the equivalence between the change in operating pressure-ratio, ΔPRO, and the loss of stability pressure ratio, ΔPRS, described in 6.4.3.1, the total loss of fan or compressor stability due to the combined distortion can be accounted for using a composite sensitivity factor, K_{COM}, defined by the equation:

$$\Delta PRS_{TOTAL} = K_{COM} \times (DP)_{COM} \quad \text{(Eq. 27)}$$

The composite sensitivity represents a weighted combination of planar-wave and spatial-distortion sensitivities and other compression-system distortion-response parameters, such as superposition, spool transfer, and spool flow-coupling factors as appropriate. Separate assessments of the effects on ΔPRS of planar-wave and spatial-distortion disturbances and their addition with the attendant problem of accounting for the phase relationships between the two forms of disturbance, are avoided in the explicit methodology (but are implicit in the composite sensitivity). In the "one-parameter" approach, the combinational algebra for accounting for the individual PRS losses is included in the dynamic-response algorithm of the engine.

A key feature of methods for assessing the effect of the combined distortion is that the range of possible planar-wave and spatial-distortion intensities is bounded by the stability margins available for dealing with the combined problem (maximum margins in the range up to approximately 30%). The problem of estimating the loss of stability of the engine is in some sense "self-limiting," enabling reasonable assessments to be made by linearized methods for engineering purposes. Insufficient information is available at the present time to assign accuracy limits to correlations, but a bandwidth of 2% ΔPRS, as suggested for spatial-distortion correlations in ARP1420 is thought to be a reasonable target.

In so far as correlation of losses of compression-system stability margin with "one-parameter" descriptors is needed explicitly, the "one-parameter" approach is regarded as being best suited to an important class of combined intake distortion problems where planar-wave frequencies are low - as for quasi-steady conditions - and where compression-system-component sensitivities appropriate to the planar wave and the spatial distortion are comparable. It can then be shown that the one-and two-parameter approaches to estimating the effects of the combined distortion on compression-system stability are equivalent. Where the sensitivities differ significantly, the frequency distribution of the planar wave, or the amplitude/frequency in the case of a simple sinusoid needs to be specified. Normally, the planar wave signature will be defined in the total-pressure distortion data at the AIP as the time variation of PFAV. The weighting assigned to the component sensitivities contributing to a datum sensitivity then becomes increasingly important as the intensity of the planar wave becomes larger in proportion to the level of the composite descriptor. An expanded form of the ΔPRS formula to include offset and superposition terms may then be required (much as for the general spatial-distortion problem when the distortion pattern is complex).

The benefits of the "one-parameter" approach are that it provides a simple and effective general method of screening mixed-distortion data by treating the unsteady total-pressure problem as a whole. It minimizes the complexity involved in formulating and processing additional descriptors at the AIP - a significant issue when multiple forms of distortion are present. It helps to resolve important questions of the time-phasing of planar-wave and spatial-distortion peaks that arise in the time-variant data at the AIP and within the engine gas path. It is consistent with the use of overall spatial-distortion descriptors, based on ARP1420 elements, developed for defining stability aspects of the distortion tolerance of the engine. As such, it is capable of dealing with waves that are concentrated in one region of the AIP.

Given that current information on the mixed-distortion problem is sparse, the "one-parameter" approach is thought to be less flexible than the "two-parameter" approach in dealing with a wide range of disturbances. When the planar-wave contribution to the overall distortion is large, exceeding declared limits of applicability of the composite method, or compression-systems are highly sensitive to either or both forms of disturbance, detailed planar-wave information to supplement the composite distortion data is indispensable. In these circumstances, the stability-accounting accuracy, linearization, superposition and phase assumptions of both methods need critical examination.

7. TESTING REQUIREMENTS

To apply the methodology presented in Section 6 to a specific system will require inlet and, if needed, compression system component/engine testing. Inlet testing defines the planar wave component at the AIP and compression system and/or engine testing defines the response to planar waves. (As discussed in 6.2, engine response can be determined by analytical or computer modeling.) Reviewing the case histories shows that the occurrence of planar waves is highly system configuration dependent. A review of the system configuration should cover any potential external sources of planar waves due to vortex shedding such as landing gear struts or external pods. The mission requirements should be reviewed to identify points where low airflow and high subsonic flight Mach numbers may lead to planar waves. Normally, buzz is designed out of the engine flight envelope, but it represents an extreme case of planar waves and should be considered with the other factors when defining the scope of a testing program to assess planar waves.

7.1 Inlet Testing

Equation 1 in Section 6 defines the fundamental inlet information required to perform a planar wave assessment. Model or full-scale inlet testing can provide this information with little additional equipment required over and above that required for time-variant spatial distortion. A review of planar wave experience indicates that the potential for planar waves is higher at low airflow and high subsonic flight Mach numbers. Therefore to capture the planar wave data, an expansion of the inlet test matrix may be required over that required for time-variant spatial distortion.

Propulsion systems in aircraft executing large rates of change in attitude (α and β) such as fighter aircraft may encounter AIP conditions at a specified attitude set (α and β) which are different than those encountered at the same attitude set with no (or small) rates of change. Possible contributing mechanisms may include transient ingestion of displaced vortices from forward structures and inlet internal separation that is affected by the motion of the aircraft. Therefore, the inclusion in the test matrix of testing with large rates of change in attitude should be evaluated based on expected occurrences of the contributing mechanisms and the availability of test capability. The effect of maneuver rate on inlet total-pressure distortion was investigated during the NASA HARV (High Alpha Research Vehicle) Program and the results are reported in Reference 2.2.9.

The effects of planar wave data requirements on the inlet tests that are conducted during a typical inlet development cycle are summarized in Figure 33.

7.1.1 Inlet Development Tests

The initial inlet development tests that are conducted are typically small-scale tests of the inlet alone (often without fuselage forebody) and are designed to be a low-cost way to study experimentally the effects of key design variables such as compression surface geometry, boundary layer control bleed system, and diffuser geometry. Because of the small scale models employed (usually smaller than 10%), only limited compressor face instrumentation can be installed. For example, a typical installation would be a four-arm, five probe-each steady-state total-pressure rake assembly with perhaps one or two high response probes for measuring RMS turbulence. These early inlet alone tests also may utilize existing flow control and flow metering equipment that is available at the test facility. Therefore, the choked flow control plug may be located some distance downstream of the AIP. This means that the diffuser volume is not correctly simulated. For these reasons, little emphasis is placed on gathering planar wave data during the initial series of inlet development tests. About the best that could be obtained, in addition to the usual inlet performance data, is an indication of the buzz limit as a function of inlet mass flow ratio. For best results, an acoustic reflection plane should be properly located to simulate the engine face. The location of the engine face in the full-scale application does act as an acoustic reflection plane for any standing waves.

After the inlet alone configuration is developed, the next step in the development process is to measure the installed inlet performance with the forebody. The inlet models employed for this testing are usually larger than 0.10 scale and have provisions for a complete 40-probe steady-state total-pressure rake assembly at the compressor face and, in addition, have a limited number of high-response transducers at the AIP to measure RMS turbulence. Some typical high response transducer arrangements are shown in Figure 34 for limited numbers of probes. These transducers can also be used to measure the time histories of the instantaneous pressures. These time histories can then be analyzed by PSD analyses to determine the existence of planar wave content. To provide realistic duct dynamic characteristics for these test runs, the primary flow control valve should be located as close as possible behind the engine face station. An example of a special type of butterfly flow control valve that was used to achieve this is reported in Reference 2.2.1. As mentioned above, the generation of realistic planar wave frequency components for internally generated disturbances depends on the simulated engine face acting as an acoustic reflection plane. The use of a suitable computer code (References 2.2.10, 2.2.11, and 2.2.12) should be considered to aid in interpreting geometric differences necessitated by the experimental configurations.

Model/Facility/Test Variables	Data	Instrumentation and Data Acquisition Requirements for Acquiring Planar Wave Data	Type and Location of Flow Control Valves for Planar Wave Data Acquisition	Test Ranges of α, β, A_e/A_c and M_o for Planar Wave Data Acquisition
Inlet Development Tests				
A. Isolated Inlet Model 1. Inlet Alone (Scale ≥ 0.1) 2. Blowdown wind tunnel 3. Mach, Inlet MFR, Geometry, Inlet B.L. Bleed Airflow	Steady-State AIP Pressures Limited Turbulence Engine Airflow, B.L. Bleed, Buzz Points	• Usually Not Required for Initial Development Tests	• No Special Requirements	• Run A_e/A_c Down to Buzz Points as Part of Inlet Performance Tests
B. Subsonic-Supersonic Inlet/Forebody Model 1. Inlet/Forebody with Fwd A/C Control Surfaces/Wing Stub (Scale > 0.1) 2. Blowdown or Continuous Flow Wind Tunnel 3. Mach α, β, Inlet MFR, Bleed Airflow, ECS Airflow, Geometry	Steady-State AIP Pressures High-Response AIP Pressures Engine, Bleed, ECS Airflows Static-Pressure Distribution	• Limited High Response Probes (≈ 4) at AIP • Use Limited No. of Transducers Avail. to Measure Amplitude and Frequency • Refer to Sec. 5.1 for Probe Locations	• Should be Near Comp. Face Station • Choked Flow Control Plug or Butterfly Vanes	• Transonic: M_o 0.085 A_e/A_c = Idle to Max α = 0 to + 10, -4° β = 0 to ± 5° • Supersonic: M_o = 1.3 to Max Design A_e/A_c = Buzz Pt to Max α = 0 to +10, -5° β = 0 to ± 5° • Low Speed: M_o = 0.0 – 0.40 WIR = Idle to Max α = 0 to +15 β = 0 to ± 10°
C. Low-Speed Inlet/Forebody Model 1. Large Scale Model (Scale ≥ 0.20) Inlet/Forebody with Fwd. A/C Control Surfaces, Wing Stub, Takeoff Doors, Nose Gear 2. Low Speed, Continuous Wind Tunnel 3. Mach α, β, Inlet MFR, Geometry	Steady-State AIP Pressures High-Response AIP Pressures Engine Airflow Static Pressure Distribution	• 40 High-Response Probes at AIP, ARP 1420 Array	• Should be Near Comp. Face Sta. • Choked Flow Control Plug or Butterfly Vanes	
Inlet Verification Tests				
A. Inlet/Forebody with Fwd A/C Control (Scale ≈ 0.2) 1. Continuous Wind Tunnel 2. Mach α, β, Inlet MFR, Bleed Airflow, ECS Airflow, Geometry	Steady-State AIP Pressures High-Response AIP Pressures Engine, Bleed ECS Airflows Static Pressure Distribution	• 40 High-Response Probes at AIP, ARP 1420 Array	• As Close as Possible to Comp. Face • Butterfly Vanes for Flow Control or Similar Choked Flow Control	• Same as Above for Similar Test Speed Ranges
Inlet/Engine Compatibility				
A. Full-Scale Inlet Model and Prototype Inlet Control, Prototype Engine and Control 1. Test Consists of 3 Phases: • Inlet Alone • Inlet Plus Inlet Control (No Engine Present) • Inlet Plus Inlet Control (Engine Present) 2. Continuous Wind Tunnel 3. Mach, Limited α, Inlet MFR, Geometry, Distortion	Steady-State AIP Pressures High-Response AIP Pressures Inlet/Engine Airflows Inlet Static Pressures Full Engine Instrumentation	• 40 High-Response Probes at AIP, ARP 1420 Array	• Prototype Engine and Control System	• Limited A_e/A_c = Sub-Idle to Max M_o = 0 – Max

FIGURE 33 - PLANAR WAVE CONSIDERATIONS FOR INLET DEVELOPMENT TESTS

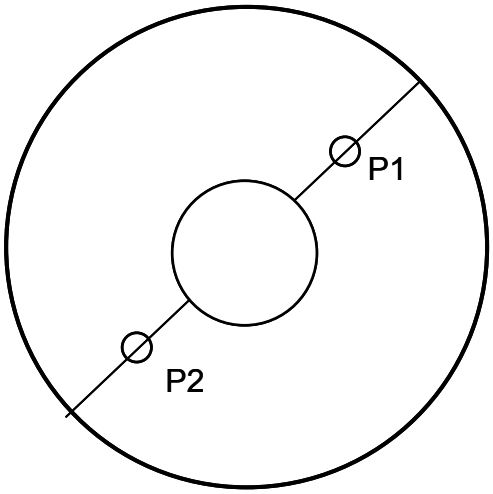

a) Two-probe arrangement for planar waves only

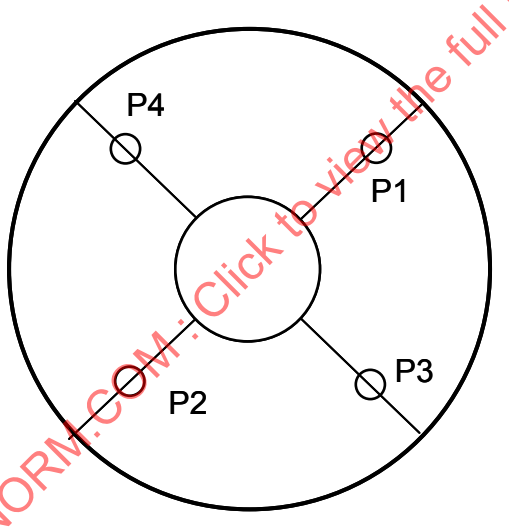

b) Four-probe arrangement for planar waves and RMS turbulence

FIGURE 34 - TYPICAL LIMITED PROBE ARRANGEMENTS

Planar waves should be investigated within the operational ranges of Mach number, inlet mass flow, and angles of attack and sideslip where aircraft requirements dictate. It is particularly important that the idle, sub-idle, and windmill airflow ranges be investigated as appropriate in the subsonic envelope(s) as air starting characteristics can be affected by the presence of planar waves. Further in the supersonic envelope, special consideration is needed for supercruise aircraft where aircraft deceleration requirements must be met by mass flow reductions to reduce thrust. (Planar waves occur at much higher mass flows ratios in this part of the aircraft envelope and represent a challenge for both the airframe and engine manufacturers to meet overall aircraft performance requirements.)

The low-speed inlet/forebody model testing is conducted using a large-scale model (~0.2) that incorporates the forward forebody and wing surfaces that can influence flow into the inlet. Other devices that can influence flow into the inlet at low speed are also simulated, if present, such as takeoff doors, nose gear, probes, and stores. The larger model scale enables the installation of a complete set of forty high-response probes at the AIP for measuring instantaneous pressure versus time histories from which PSD analysis can be used to determine planar wave content. A full range of low-speed angles of attack, sideslip, and Mach numbers from zero up to approximately 0.40 should be tested.

After development of the inlet is completed, inlet verification tests are accomplished with a large-scale (>0.20) inlet/forebody model that incorporates forty high-response probes at the AIP. This model is tested over the complete subsonic/transonic/supersonic Mach number range, α and β range, and range of inlet mass flow ratios to verify the inlet performance, distortion, and flow stability characteristics at all key operating points. The AIP instrumentation is similar to that used for the 0.20-scale low-speed model.

The full-scale inlet/engine compatibility test of Figure 33 utilizes a prototype inlet control and a prototype engine and control. A full-scale array of forty high-response probes is used at the AIP. Because a complex support system and installation hardware are required for the full-scale inlet and engine, only a limited range of angles of attack and sideslip is possible. The verification test might also be accomplished in full-scale flight testing.

7.1.2 Engine and Compression System Testing

A number of methods have been used in an attempt to obtain the response of a compression component to a periodic variation in inlet conditions. Selected methods are discussed further in Paragraph 7.2.

Past methods for obtaining the response of a compression system or an engine have required generating a near sinusoidal input of total pressure at the inlet to the compression component or engine and determining its stability limit at each frequency of interest. Based on one set of test data (Reference 2.2.5), the desired frequency range should cover from as close as is practical to 0 Hz to a frequency slightly in excess of the one-per-rev frequency equivalent of the rotational speed of the fan or compressor.

It is recommended that an instrumented engine test be conducted in a controlled environment to verify this methodology using planar waves over the sensitive frequency range with the following frequency content:

1. Pure sinusoidal
2. Harmonic
3. Random
4. Random plus sinusoidal or harmonic

With data from these tests, the validity of proposed procedures can be verified and complementary computer simulations can be substantiated.

It is further recommended that some of the above planar wave tests be accomplished simultaneously with spatial distortion to determine if the spatial and planar wave stability margin losses are directly additive as has been assumed in the analysis of this report and what the values of the coupling coefficients are.

7.1.3 Instrumentation

The standard 40-probe AIP instrumentation array described in References 2.1.1.1 and 2.1.1.2 is more than adequate to define the planar wave amplitude and frequency. If planar waves were the only item of interest on a particular test, then a smaller number of high response probes distributed over the AIP may be sufficient, since by definition a planar wave affects the entire AIP and the cross-correlation function or phase relationship between probes should be high. As noted previously, a significant consideration in the configuration of the inlet test is the proper simulation of the engine acoustic reflection plane. Case History A shows an instance of planar waves occurring at a frequency which corresponds with open-closed organ pipe theory. The resonant frequency is dependent on the length of the pipe from the cowl lip (open end) to the engine face (closed end) that leads to the requirement for simulating the acoustic reflection plane. A flow-measuring plug downstream of the AIP in an inlet test serves this purpose and should be located as near as practical to the engine acoustic reflection plane. If the flow plug is choked, the inlet will be isolated from downstream disturbances. These disturbances would otherwise be sensed by the AIP instrumentation and lead to invalid conclusions about inlet disturbances both in frequency and amplitude.

7.1.4 Data Processing and Screening

The first step in processing the inlet data is to obtain the time-varying spatial average of the AIP pressures using Equation 1 of Section 6. The time-variant spatial average becomes the input to a Power Spectral Density (PSD) calculation. The PSD will identify frequencies where planar wave activity is occurring. All of the guidance in Section 6 of Reference 2.1.1.2 concerning data processing would apply to the planar wave data processing. A schematic of the inlet data process from the AIP pressures to the PSD determination is shown in Figure 35.

The data processing must enable time-synchronous traces of average total-pressure and spatial distortion descriptors or descriptor elements to be derived in a form suitable for combinatorial analysis. Test arrangements need to take into consideration the duct-outlet termination to assure correct simulation of the inlet length/volume dynamics. Data scaling uses constant Strouhal number (see also ARP1420, 7.1)

The inlet test data must be screened in a coordinated program that involves the airframe company and the engine company. This screening will determine whether significant planar wave activity is present that could create flow stability problems for the engine. The airframe company will provide measured high-response total-pressure data at the AIP and the engine company will provide sensitivity criteria, which can be used to determine the response of the engine to the type of planar wave activity present.

7.2 Compression System Component Testing

The results of the inlet test will determine the matrix of frequencies, amplitudes, corrected flow and speed ranges over which the compression system may be tested. For multi-spool compression systems, a transfer function for the upstream component will be required to define the proper inlet conditions for each downstream component. Inlet and exit wave forms need to be measured.

To conduct a test of this scope with a single planar wave generator could be extremely difficult. A combined experimental/analytical approach may be appropriate in this case. With the availability of the one-dimensional transient compressor model, the test program can be designed to validate the model predictions at certain points and then the model would be exercised to generate the full sensitivity curve and the transfer characteristics. This is the approach used in Reference 2.2.5.

The methodology of Section 6 is a general methodology capable of assessing any and all planar waves present in the inlet data. If analysis of the inlet data justifies a simplification of the methodology to deal with a few significant frequencies, the compression system component testing could also be simplified. A planar wave generator could be selected or designed to meet the specific requirements of the program and to avoid the limitations of these devices when trying to use them over a wide frequency range.

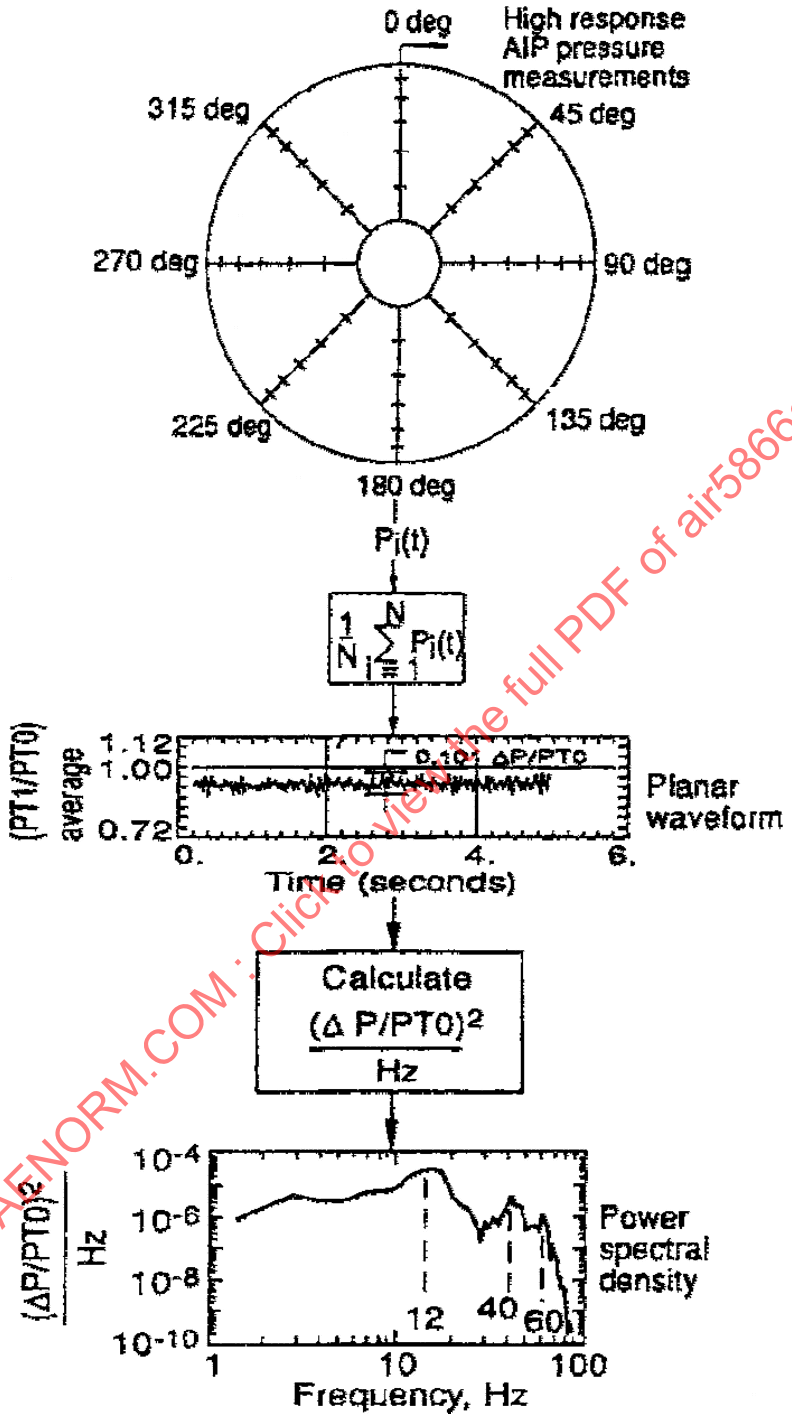

FIGURE 35 - PLANAR WAVE INLET DATA PROCESS

7.2.1 Planar Wave Generators

The methodology of Section 6 requires a sensitivity (K_p) as a function of frequency to assess the stability impact of planar waves. The K_p generated from a fan test conducted during the early 1970s is shown in Figure 36 (same as Figure 22, repeated here for convenience). In this test, a device called the Planar Pressure Pulse Generator (P^3G) was installed upstream of the fan rig to produce the planar waves. The device consisted of a perforated rotor and stator (see Figure 37). By varying rotor speed, the frequency can be varied, and by changing the rotor to stator spacing, the amplitude is varied. Note that there are no data below 40 Hz due to mechanical resonances. A similar concept consisting of a spoked rotor and spoked stator was tested at frequencies above 78 Hz (Reference 2.2.13, see Figure 38). Various levels of blockage were tested and the effects of attenuation with axial distance downstream of the device were investigated. It was discovered that planarity of the wave increased for some distance.

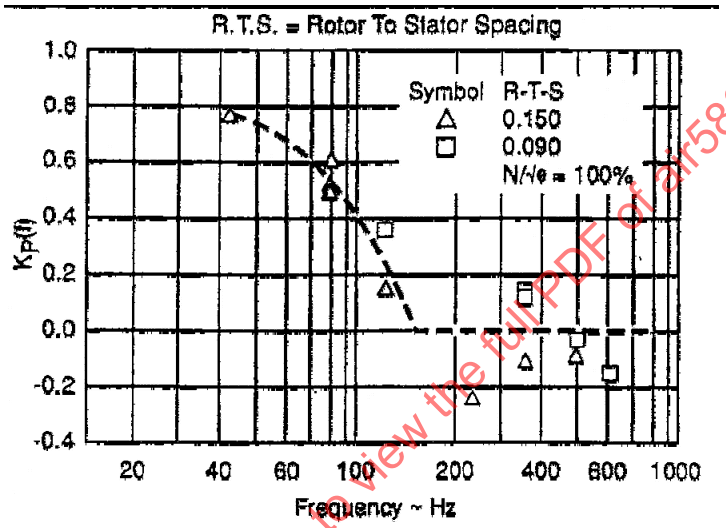

FIGURE 36 - DYNAMIC DISTORTION SENSITIVITY VERSUS FREQUENCY - N/√θ = 100%

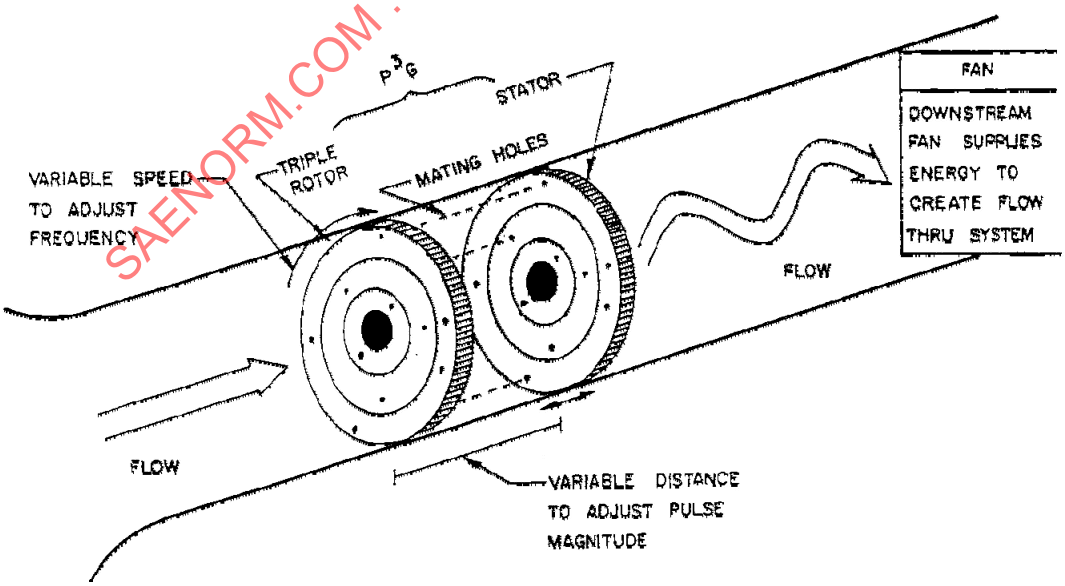

FIGURE 37 - ROTATING PERFORATED DISK (GE AND NASA)